NON-INVASIVE BLOOD GLUCOSE MONITORING OF 95% CERTAINTY BY PRESSURE REGULATED MID-IR

By

Yuanzhe Chen, B.Eng.

A Thesis

Submitted to the School of Graduate Studies

in Partial Fulfilment of Requirements

for the Degree

Master of Applied Science

McMaster University

Dec. 2018

MASTER OF APPLIED SCIENCE (2018)

McMaster University, Hamilton, Ontario

Faculty of Material Science and Engineering, Engineering Graduate Program

TITLE:	Non-invasive blood glucose monitoring of 95% certainty by pressure regulated Mid-IR
AUTHOR:	Yuanzhe Chen, B.Eng. (Shandong University)
SUPERVISOR:	Dr. Gu Xu
COMMITTEE MEMBERS:	Dr. Igor Zhitomirsky Dr. Joey Kish
NUMBER OF PAGES:	II, 59

ACKNOWLEDGMENTS

I am deeply grateful to my supervisor Dr. Gu Xu for his unforgettable encourage and countless support in my research work. He spares no effort to teach me not only about how to do research but also about how to be a better self. Thank you so much for offering me such a precious opportunity. I have learned a lot from you during this remarkable journey but I know that it is far less than one percent of what you try to teach me.

I would also like to thank Dr. Qi Zhou for the help of my research work. Despite her unimaginably busy schedule, she always had time and patience to help me and guide me through my research journey.

I appreciate my colleagues and all the friends who supported me during my graduate studies. Thank you, Ryan T. Wang and Edward G. Tai, for your inspiring discussion with me and invaluable friendship.

I really appreciate my committee members for their time and patience. And also, I want to give my thankfulness to all the professors who have instructed me on the research and courses, the technicians and staffs who have helped me on my study.

Last but not least, I would like to thank my parents for supporting me, encouraging me and trusting me. I can always be inspired by you no matter how much I get discouraged. Thank you so much. I miss you.

Table of Contents

List of Figures

List of Tables

List of Abbreviations

Mid-IR	**Mid-Infrared**
NIR	**Near-Infrared**
IR	**Infrared**
FDA	**Food and Drug Administration**
DM	**Diabetes Mellitus**
BG	**Blood Glucose**
WHO	**World Health Organization**
FGT	**Fasting Glucose Test**
OGTT	**Oral Glucose Tolerance Test**
CGM	**Continuous Glucose Monitoring**
ISF	**Interstitial Fluid**
ATR	**Attenuated Total Reflection**
FTIR	**Fourier-Transform Infrared Spectroscopy**
MCT	**Mercury Cadmium Telluride**

Abstract

To fight against diabetes mellitus, a chronicle metabolic disease, from which more than 400 million people suffer in the world, the patients have to puncture their fingers 4-5 times a day when using a glucometer for the blood glucose level checks, causing invasive pain and the risk of infection. Therefore, the non-invasive method has been urged for blood glucose monitoring, among which the mid-infrared spectroscopy (Mid-IR) response of interstitial fluid was found to be promising. However, despite the prolonged effort, the accuracy still falls well below the FDA's requirement. To break this barrier which lasted for almost three decades, we discovered the finger contact pressure playing a critical role during the measurement, where the Mid-IR reading could be affected significantly by a small change of the finger posture. In addition, the Mid-IR absorption level was also found to be highly associated with individuals, revealing the necessity of adjusting the calibration correlation for each patient. By imposing a certain contact pressure monitored by a pressure transducer, we were able to achieve over 95% certainty from the Mid-IR measurement of glucose concentration and 100% comparability to the "true" glucose concentration for the first time. This significant enhancement of the accuracy was found to be mainly attributed to the fact that, the finger tissue undergoes certain morphological change because of the pressure, where much more interstitial fluid becomes accessible by the Mid-IR detector.

1 Introduction

Diabetes mellitus (DM) is a long-term metabolic disease in which the body cannot produce or respond to the hormone insulin, resulting in blood glucose concentration varies beyond the normal range (Renard, 2005). It's a complex disease, with potentials of affecting nearly everybody organ through complications. It may lead to serious complications such as hearing impairment, cardiovascular diseases, nerve damage, and kidney damage etc. Studies have shown, however, that these complications can be prevented with close monitoring and control of blood glucose (BG) level since the late 60's of last century (O Connell, 2006). Glucose, which acts as the energy source in biological cells, can be decomposed by insulin, a hormone secreted by the pancreas (Renard, 2005 & Tao, 2015). Unfortunately, close monitoring of blood glucose is difficult to attain with current "finger-prick" technology, which involves puncturing the skin (usually at the tip of a finger) to obtain a drop of blood (Saptari, 2004).

According to WHO, diabetes is becoming an increasingly serious health threat all over the world. The diabetes patients are expected to rise up from 170 million in 2000 to 365 million by 2030 (WHO, 2016). Aguiree et al (2013) estimated that there are 382 million adults were suffering from DM in 2013 and predicted a 55% increase in the number of people that may have DM for the next 25 years, as shown in Figure 1. Risérus et al (2009) reported that 548 billion USD (11% of total expenditures on healthcare worldwide) is spent on DM control and treatment in 2013 and expected these

expenditures to increase to 627 billion USD in 2035. These rising figures prove that DM is an increasingly serious global problem that would cause a huge financial burden to the society. Therefore, regular monitoring of BG is of great importance in preventing diabetes and reducing budgets.

Fasting Glucose Test (FGT) and Oral Glucose Tolerance Test (OGTT) are often used to confirm the onset of DM (Baehr, 1994). However, DM patients are required to monitor their BG level at least 4-5 times/day to avoid any hyperglycemic/hypoglycemic events (Chase, 2010 & Yadav, 2015), which means these tests are not appropriate for the patient because they are not for frequent use. Thus, more and more techniques have been developed for glucose monitoring, some of which will be discussed below.

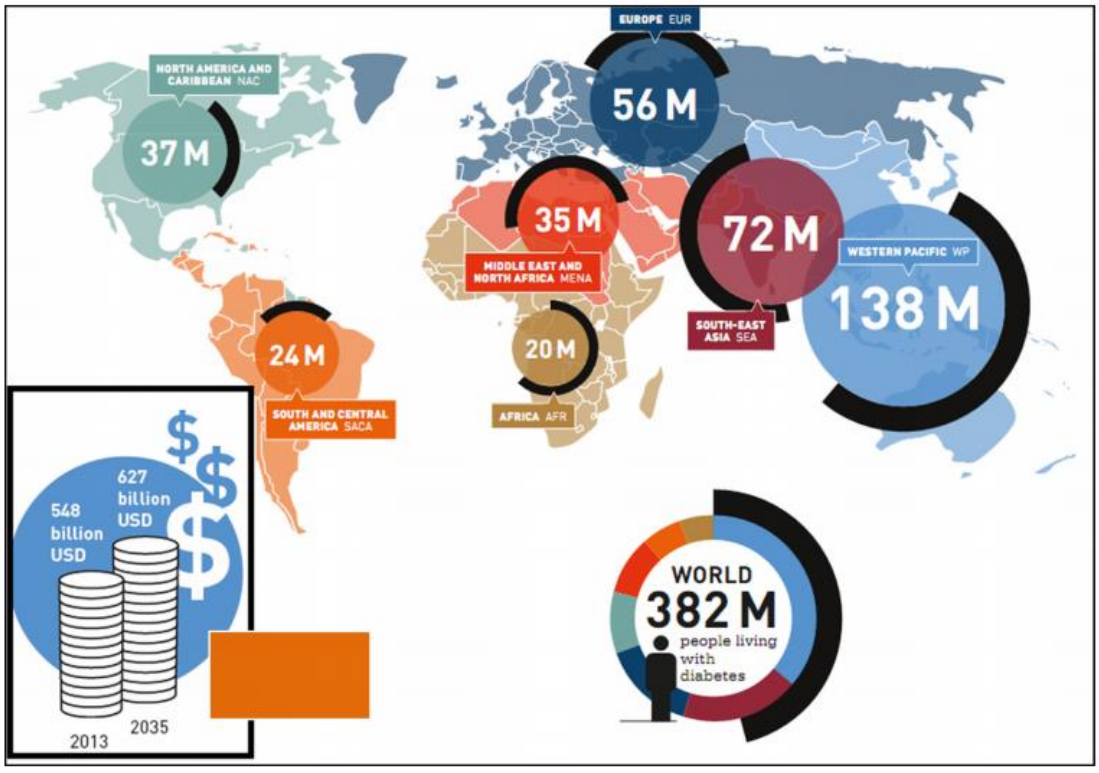

Figure 1 Number of diabetic patients worldwide (Aguiree et al, 2013)

2 Literature Review

Current glucose monitoring techniques include invasive, minimal-invasive and non-invasive method depending on their transduction mechanism. Details are elaborated below.

S. no.	Method	Type of method	Sample/continous
1	Invasive method	Finger stick	Sample
2	Minimal invasive	Subcutaneous implanted biosensors	Continous
		Iontophoresis, microdialysis, sonophoresis	Continous
3	Non-invasive	Sweat, saliva, tears, urine	Sample
		Raman spectroscopy, optical coherence tomography, polarimetry, photoacoustic, ultrasound, bio-impedance spectroscopy, mid-infrared spectroscopy, near-infrared spectroscopy	Continous

Figure 2 Various glucose monitoring methods

2.1. Invasive Method

Invasive blood glucose devices are most widely used. This method involves piercing the finger skin or other areas to draw a tiny amount (around 50 μL) of blood, which is then transferred to a testing strip paper for estimation of BG level (Rhee, 2007). This can be achieved by optical, chemical or electrochemical methods. Clearly, repeated piercing and drawing work is painful and may cause infection. Furthermore, enzyme-based one-time strips can be somewhat expensive which would limit its application. Figure 2 below shows a normal conventional invasive BG monitoring device.

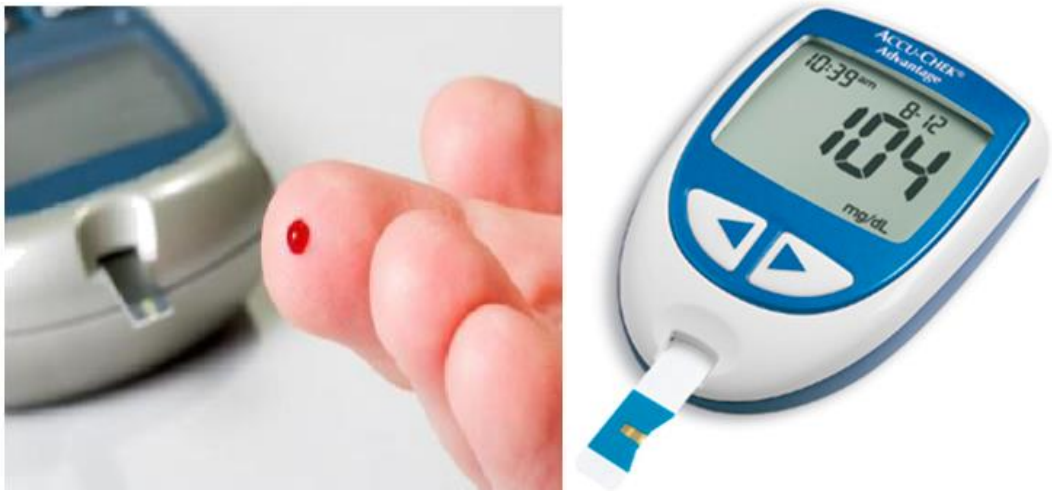

Figure 3 Commercial invasive glucometer (Yadav,2015)

One other drawback of this technique is its discrete measurement of glucose which means an episode of hyper/hypoglycemia can be neglected during sleep or driving (Heinemann, 2003). Therefore, researches in minimal-invasive or non-invasive devices

which monitors BG level continuously are of huge significance and have been developed with effort. When life-threatening events occur at any time, patients will be alerted by the devices, dubbed Continuous Glucose Monitoring (CGM). CGM enables the analysis of BG level trends and helps the management of DM. It provides the human body glucose information every 10 min around and gives alerts at any hyper/hypoglycemia events even at midnight (Buckingham, 2005). Nevertheless, the accuracy of CGM devices still needs to be improved.

2.2 Minimal-Invasive Method

The minimal-invasive device causes minimal injury to human skin which consists of several layers (Rhee, 2007). Heinemann et al (2003) have already reported several techniques including sonophoresis, microdialysis, iontophoresis and an implantable subcutaneous biosensor which only cause negligible damage to the skin. All these devices measure the glucose level in Interstitial Fluids (ISF), and studies have proved the BG level is the same as that in ISF under steady state condition (Bolincier, 1992).

Subcutaneous measurement uses biosensor implanted beneath the skin to conduct the measurement in ISF, which is controlled by radio frequency or optical methods (Renard, 2008). The main drawback of such a device is the lifetime (only a few days) and glucose level lag (few minutes) which limits its use. When a small amount of electrical current passes through the skin and causes ions and ISF to migrate, dubbed reverse iontophoresis or iontophoresis (Tura, 2007). Such devices can cause skin irritation and

skipping measurement because of body temperature, sweating and physical activities (Park, 2009). Glucowatch produced by Cygnus Inc. is a typical example which is now withdrawn from the market due to inaccuracy and skin irritation. Microdialysis method measures the glucose level in ISF by implanting a fine hollow fibre beneath the skin. Such a method gives precise results, yet it is still not being commonly used because of the high instrumentation cost and its bulky size (Heinemann, 2003 & Park, 2009). For sonophoresis technique, low frequency ultrasonic wave is applied to improve the skin permeability which helps the extraction of ISF. Such ISF is then analysed externally via optical or electrochemical glucose sensor (Chuang, 2004). These minimal-invasive devices are not optimum for continuous BG monitoring either because of their short lifespan or because of drift and stability problems. Hence, a massive number of researchers are working to develop new techniques for non-invasive BG monitoring.

Figure 4 Commercial minimal-invasive glucometer (Yadav,2015)

2.3 Non-invasive Method

Almost all commercially available glucometers involve prick the fingertip of patients for blood sampling, and the patient needs to sample their blood for at least 4 times a day which is painful (Vashist, 2011). Hence, the development of non-invasive technology is the only way to achieve pain-free monitoring for DM patients (Tura, 2007 & do Amaral and Wolf, 2008). And there is a rapidly increasing number of publications in this field, as indicated in Fig. 5.

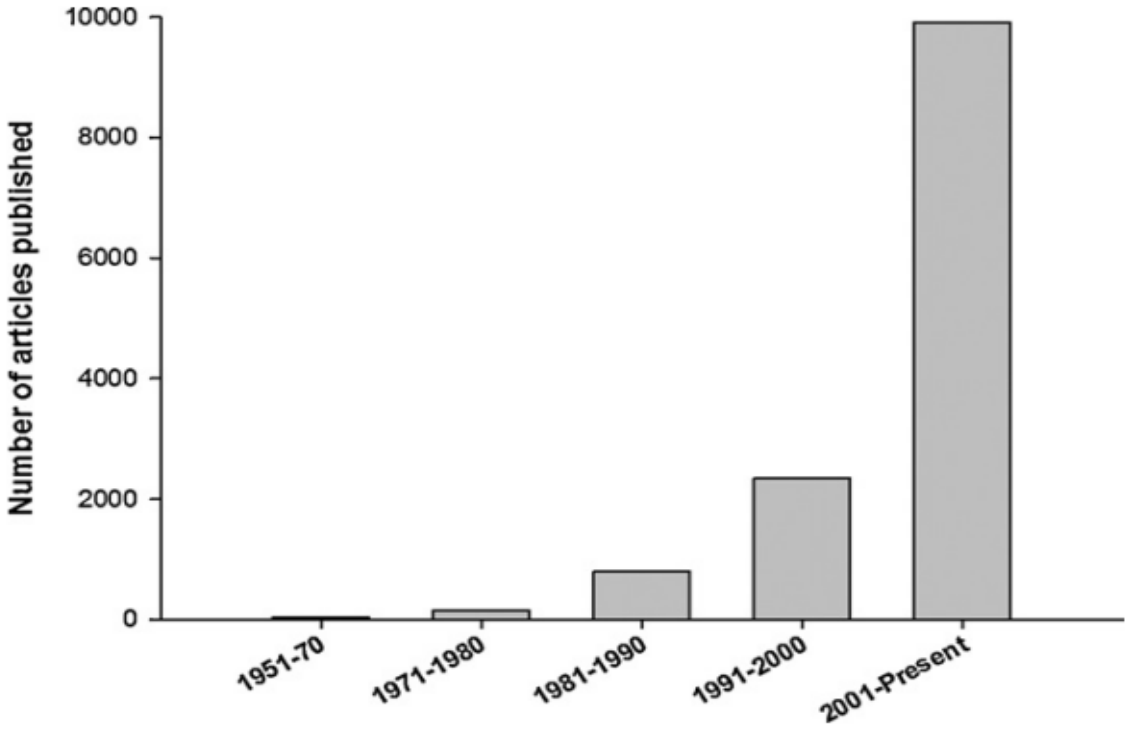

Figure 5 Number of articles published since 1950

Christiansen (2013) reported the application of bioimpedance spectroscopy for BG monitoring which measures tissue impedance by alternating current. However, the

device is strongly affected by water content and disease state which would affect the cell membrane. Meanwhile, Gasim (2013) reported thermal emission spectroscopy which measures infrared (IR) signal emitted by human body owing to BG level variation. Although this technique demonstrated good reproducibility for glucose monitoring, the strong influence from body temperature and movement greatly limited its spread.

2.3.1. Bio-impedance spectroscopy

The bio-impedance spectroscopy uses an alternating current passing through body tissues and then measures the impedance of such tissue which is influenced by the composition of the tissue (Khalil, Mohktar, and Ibrahim, 2014). The spectrum is normally measured within the frequency range from 100Hz to 100MHz. The variation of glucose level in plasma will lead to the varying Na+ and K+ concentration and consequently result in red blood cells (RBCs) membrane potential change (Christiansen, 2013). Such potential change is then detected by the impedance spectrum and ultimately gives the glucose concentration (Eikje, 2007 & Block, 2008). However, the device is strongly affected by water content and disease state which would affect the cell membrane.

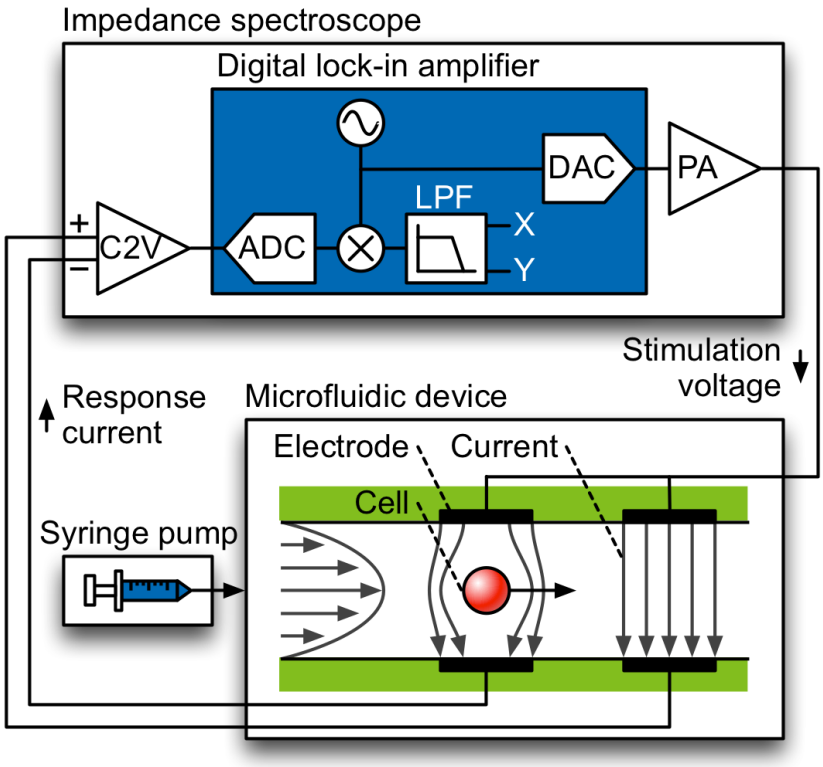

Figure 6 Bio-impedance spectroscopy (Khalil, Mohktar, and Ibrahim, 2014).

Pendra® is a glucose monitoring wristwatch uses this technique from Pendragon Medical Ltd., Switzerland. It was approved by FDA in 2003 and has been used to detect glucose change trends. It was designed for specific people with local dielectric skin that has a minimum resonance frequency (Pfützner, 2004). Pendra is no longer available in the market as the company went bankrupt in 2005. But the research in bio-impedance spectroscopy is still being conducted by Solianis Monitoring AG, Switzerland.

2.3.2 Thermal emission spectroscopy

This is a technique that measures the naturally emitted infrared (IR) signals by the human body due to glucose level variation (Gasim, 2013). Malchoff et al (2002), Khalil et al (2001) and Yao et al (2011) measure the forearm, fingertip and ear respectively, using such a technique. Chu et al (2011) reported an absorptive effect of glucose on IR radiation and stated that the absorption is directly related to glucose concentration. Yao et al (2011) proved tympanic membrane is the best for glucose monitoring because the signal only needs to cross small path length. Although this technique demonstrated good reproducibility for glucose monitoring, the strong influence from body temperature and movement greatly limited its spread.

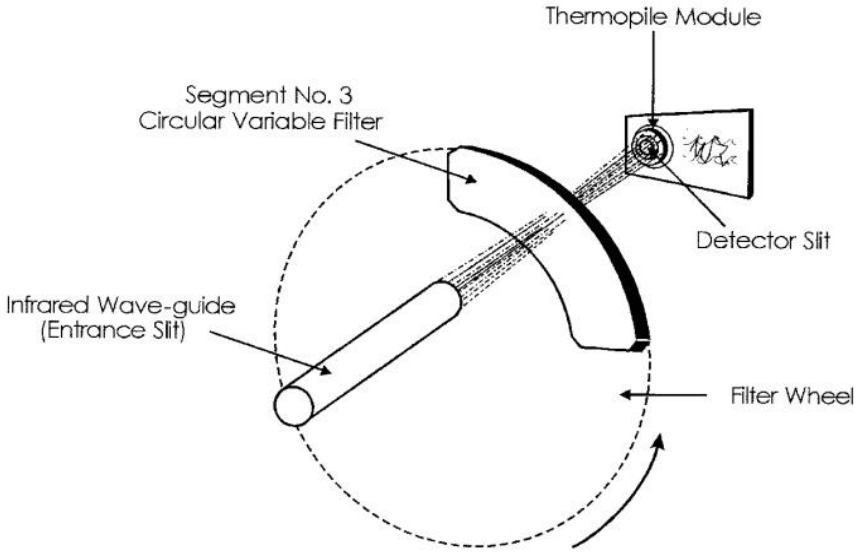

Figure 7 A typical thermal emission spectroscopy (Malchoff et al, 2002).

2.3.3. Raman spectroscopy

Raman spectroscopy measures the light scattered by transparent sample which has lower energy and intensity compared with the original light from visible to MIR region (Ellis, 2006). The biggest merit of this technique is its narrow and distinct peak and its resistance to water influence (Park, 2009). However, it needs a long spectrum acquisition time and the laser intensity and wavelength are unstable. Ergin et al (2005) used an optical fibre to focus 785 nm beam to receive the results which lead to another problem. Since the glucose concentration is measured by the Raman signals in MIR range scattered by aqueous humor, the potential photothermal damage to eyes has to be investigated before such techniques being applied in human (Chuang, 2004).

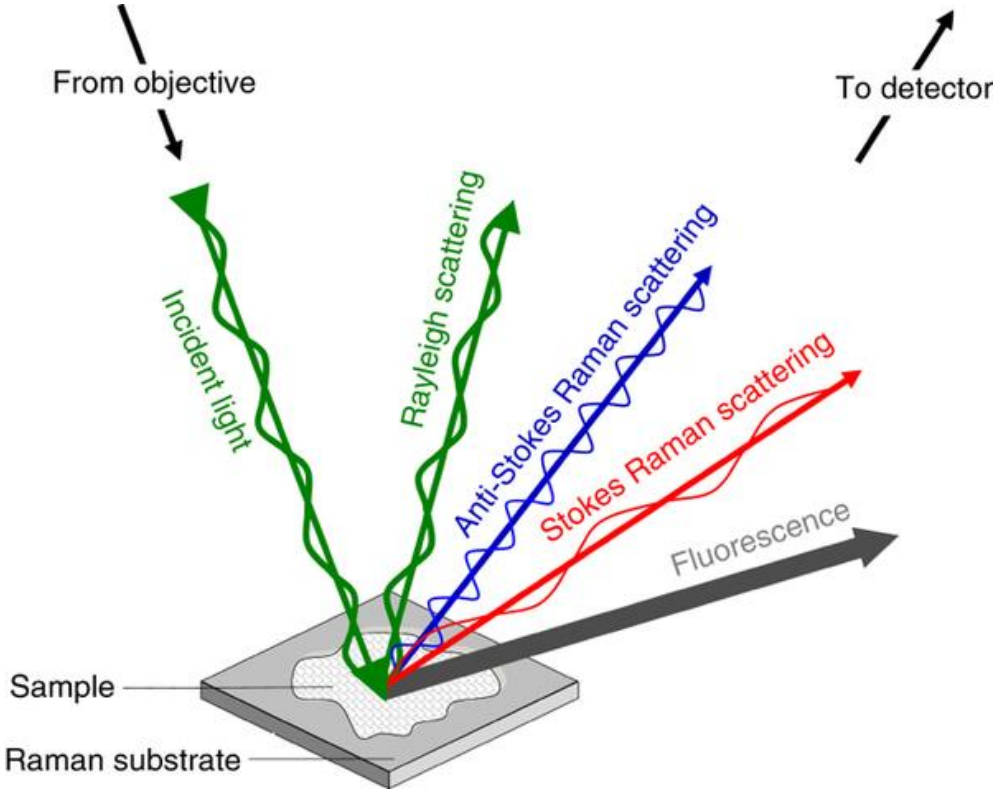

Figure 8 The principle of Raman spectroscopy (Ellis, 2006).

2.3.4. Photoacoustic spectroscopy

When laser beam interacts with tissue cell, heat will be generated, and it would emit acoustic signal, dubbed photoacoustic. Photoacoustic spectroscopy is a device that uses a piezoelectric sensor to monitor these signal (Steil, 2003). At a specific wavelength, selective BG detection can be achieved by this method, which gives the benefit of water-resistance (Allen, 2005). A spectrum can be generated by varying the wavelength from

ultraviolet to NIR region. But, such device is sensitive to environmental parameters, such as temperature or pressure change, and influence from physiological substances (Wickramasinghe et al, 2004). Currently, this technique is being applied in Aprise, a BG monitoring product in Glucon company. Aprise has good BG level correlation, but it is strongly influenced by physiological substances.

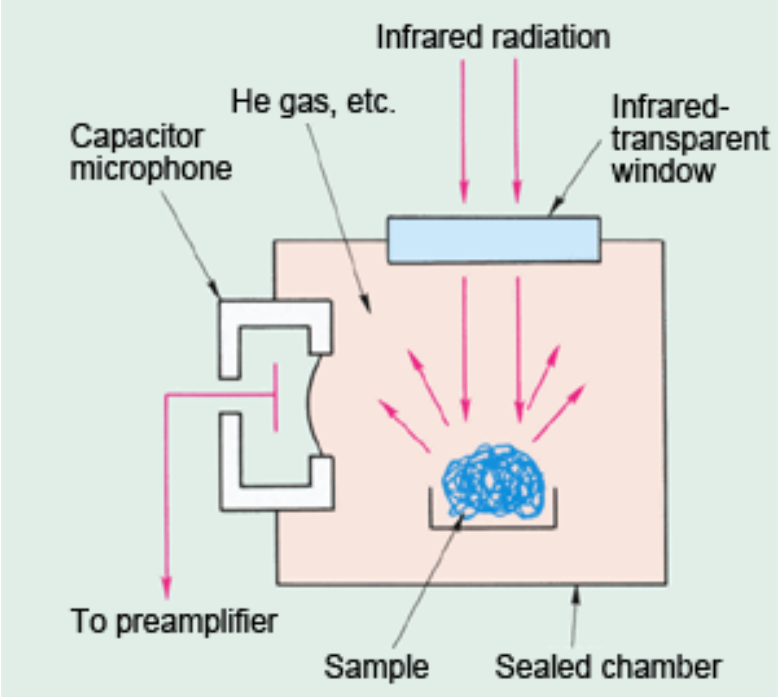

Figure 9 A typical Photoacoustic spectroscopy (Steil, 2003).

2.3.5 Near-infrared spectroscopy

NIR refers to the light within the wavelength range of 750-2500 nm. NIR spectroscopy is a device that uses a light beam within such range to focus on human body

to measure the BG level (Vashist, 2012; Barman, 2011). This is achieved by calculating the variation in light intensity owing to reflection and transmission in the tissue. The amount of light intensity variation is related to the glucose concentration which influences the absorption and scattering properties of tissue. Since water content in human tissue is way much larger than that of glucose, the absorption contributes from glucose is extremely low, which means the glucose signal constitutes only approximately 0.001% of the overall signal (Barman, 2011). Hence, the glucose spectral bands are overlapped by the strong NIR signal from water, fats, proteins and hemoglobin.

So far, NIR spectroscopy experiments have been conducted in earlobe (Malin, 1999), finger-web (Maruo, 2003), finger cuticle (Sibbald, 1996), forearm (Monnier, 1999), oral mucosa (Whiting, 2011), lip mucosa (Guariguata, 2011), tongue (Oomen, 2002), nasal septum (Cunningham, 2010), cheek (Kasemsumran, 2006) and arm (Schrader, 2005). Among these results, data measured from inner lip gives good correlation with BG with only a few minutes time lag. However, this technique is seriously influenced by skin hydration, blood pressure, concentrations of triglyceride and albumin and other physicochemical parameters (Renard, 2008). In addition, it is also sensitive to environmental conditions such as humidity, atmospheric pressure, carbon dioxide and temperature variations. The results are affected by skin thickness (Wentholt, 2005), and the disease states such as hyperglycaemia and hyperinsulinemia (Vaddiraju, 2010). All these limitations make NIR spectroscopy a bad candidate for Non-invasive glucose monitoring devices.

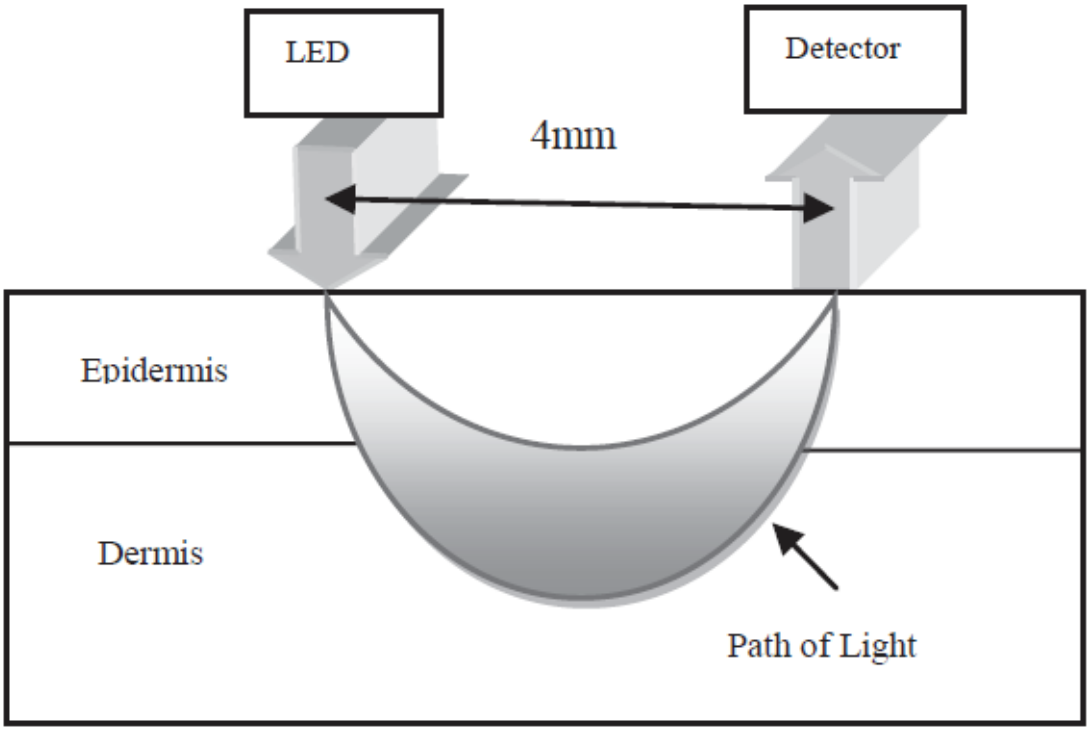

Figure 10 Schematic of cross section area of skin layers and NIR light path (Barman, 2011)

2.3.6 Mid-infrared spectroscopy

MIR spectroscopy has the similar working principle with NIR spectroscopy but its beam light varies within the range of 2500–10,000 nm (Shen, 2003; Khalil, 2004; Roychoudhury, 2006). Compared with NIR, MIR has reduced scattering but increased absorption properties owing to higher wavelengths (Tamura, 2004). Among the many candidates, infrared spectroscopy (IR) has been considered as the most promising, employing either near-infrared spectrum (NIR) or mid-infrared spectrum (Mid-IR).

Although NIR spectroscopy has a penetration range up to 50mm in human tissues, which enables direct detection of glucose level in the capillary, the absorption of glucose in the NIR wavelength is very weak, even below that of water in human tissues, leaving the absorption peak swamped by the water peak12. On the other hand, Mid-IR out-performs in that regard, due to its longer wavelength giving rise to a sharp and strong peak of glucose. Nevertheless, despite the long-term effort in Mid-IR, none meets the in-vivo accuracy required by the FDA to date (Kruse-Jarres, 1990; Yao H., 2007; Chu M.X., 2011).

The long battle dates back to the early 90s, when studies were conducted to observe the Mid-IR spectra of nasal, mucus, tears and even body parts of mice17 to aim for the prediction of the glucose level. For example, Yao et al and Chu et al reported an embedded sensor on contact lenses for in-situ tear glucose assessment (Yao H., 2007; Chu M.X., 2011). Iguchi et al demonstrated a wearable biosensor for tear glucose measurement (Iguchi, S., 2007). But none of these were able to produce reliable non-invasive glucose data, due mainly to the poor correlation between either nasal, mucus or tears and the blood sugar level. More recently, interstitial fluid (ISF) under the shallow skin layer was found to possess a strong correlation with blood glucose, based on which Kino et al developed an attenuated-total-reflection (ATR), Mid-IR spectroscopy system with hollow optical fibres to measure the blood glucose level at the inner lip area, and reached an accuracy of 80% (Kino S., 2016) Better still, Liakat et al developed a quantum cascade laser system to measure the blood glucose level on the palm and employed both partial least squares regression (PLSR) and derivative spectroscopy techniques for the

data processing, presenting an improved accuracy up to 84% (Liakat S., 2014). Although this is better than other experiments which were mostly under 80%, it still falls below the minimum requirement of FDA, which has been the major barrier for the last 28 years.

It is therefore the purpose of the current study, to overcome this barrier by a traditionally ignored variable, which was revealed during the countless experiments and the literature survey, when we discovered the finger contact pressure to be a significant factor on the Mid-IR measurement accuracy. Through schematically designed experiments we confirmed that, the contact pressure of the glucose sensor applied on human finger bears a strong correlation to the glucose measurement data. As a result, one only needs to add a pressure transducer to sense or control the contact pressure, in order to obtain a much improved accuracy. When this contact pressure is maintained at a certain level, we are able to achieve 95% certainty on the blood sugar measurement and 100% comparability to the "true" glucose concentration, achieving at last the FDA target in a completely non-invasive fashion.

3. Experimental and data analysis method

3.1 Experimental work

Simulating many published ISF measurements by Mid-IR (Smith,1992; Knapp, 1996; Hoenig, 1996), the experimental setup includes an FTIR spectrometer (Nicolet 6700, Thermo Fisher Scientific , USA) with a mercury cadmium telluride (MCT)

detector and an attenuated total reflection (ATR) ZnSe prism of 5mm size. Due to the consideration of the potential damage of the infrared and the chemical properties of the ATR prism, the fingertip of the index finger was considered to be the tested position. To accommodate the newly recognized variable, a sensitive pressure transducer made from piezoelectric materials（FSR400, Interlink Electronics, USA） was placed under the fingertip, next to the ATR prism, which is close enough for a precise contact pressure reading. When volunteers put their fingers on the top of the ATR prism, due to the change of the refractive index, infrared beam could transmit into the finger tissue and then reflect to the detector, carrying the information needed. Each ATR spectrum in vivo of a participant's middle finger was averaged by 16 scans in the spectral regions of 800 cm−1 - 1600 cm−1, when the room temperature fluctuated between 25-26℃, and the instrumental resolution set at 4cm-1. The time needed to record a spectrum was about 12 seconds, short enough to maintain a constant finger pressure. Before the test, the spectrometer needs to scan the background spectrum of the ATR prism once, because the ATR prism itself has own absorption. The figure below shows examples of the absorption of different ATR prisms.

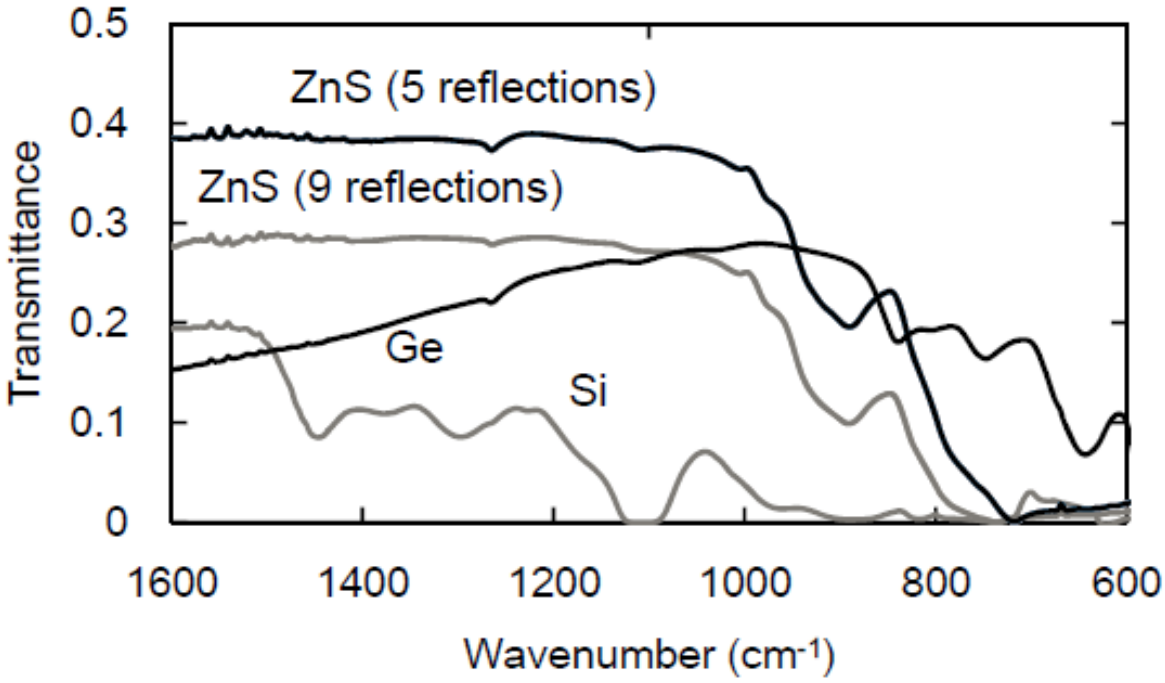

Figure 11 Examples of the absorption of different ATR prisms (Kino S., 2016)

As a pilot study of a new method, before the further scale-up, 6 subjects were recruited, as being practiced in the literature (Liakat et al; Iguchi et al; Haxha et al; Yadav et al; Eikje et al). All of the participants are normotolerant, as has been the case in other studies (Yadav et al; Liakat et al). The middle finger of each participant was sanitized beforehand using the ethanol solution. The blood glucose level of each participant (normotolerant) was varied by consuming 30g jelly beans and measured again after 30 minutes. After the background calibration, we measured the blood glucose absorption spectra at 3 different pressure levels of 20, 5 and 0.1 N/cm2, monitored by the pressure sensor, which incurs a possible error of less than 2%. For each participant at

each pressure level, 3 observations corresponding to the reference blood glucose levels were read. The reference blood glucose level was measured invasively by glucometers (OneTouch Ultra, Lifescan Inc.), USA and 3 glucometers were employed together to confirm the invasive data of the blood glucose level, to ensure the accuracy of the standard reference. Participants need to raise their fingers up after each measurement and wait for at least a minute, or gently massage their fingers to speed up the recovery of the finger tissue before the next measurement.

3.2 Data analysis method

Since the 1080cm-1 peak heights (M) in the Mid-IR is mainly attributed to the blood glucose absorbance, we expect a linear relationship between the peak heights (M), and the glucose concentration in vivo (C), via M=KC, where K is the association coefficient that is unknown and needs to be estimated. A constant K (a zero uncertainty of K) would represent a perfect, one-to-one mapping between the Mid-IR reading (M) and the "true" blood glucose variation (C) which suggests a 100% accuracy of the Mid-IR method.

Given the experimental data of M and C, the constant K can be estimated by the mean of Ks which is calculated by M/C. Due to the human skin variations, the actual K value could differ tremendously from one person to another and, therefore, is subject dependent. To overcome this problem, we determined the accuracy, or certainty of the Mid-IR technique by D, the percentage uncertainty of K, as given by the equation:

$$D = |K_i - \overline{K}|/\overline{K} \quad (1)$$

This criterion becomes subject independent and it is, therefore, only meaningful to use the percentage uncertainty of K, or D as a means to assess the accuracy of the new method in our experiments. The approach of analysing D, the percentage uncertainty of K here, gives a more straightforward way of obtaining percentage uncertainty, which can be translated directly to picture the accuracy, rather than the usual approach found in the literature, where the K values were first obtained at one glucose level, and employed subsequently to be "fitted" with the "predicted" M at other levels. Compared with their analysis between glucose concentration and absorption, we analyzed the K, the correlation coefficient of the glucose concentration and absorption under various pressures directly. And we defined the accuracy by the uncertainty of K, which gives a more direct explanation of the influence of various contact pressures.

According to the FDA's requirement, a variation within a 95% confidence interval of ±15% from "true" blood glucose concentration measured by C is acceptable if using M to predict C. It translates the 95% confidence interval of K to the range of (0.8696K, 1.1765K). From Eqn. 1, it also implies an acceptable range of <13.04% or < 17.65% for D, when the observed K is less or greater than the mean value of K, respectively. In other words, it will be acceptable by FDA if the observed D ranges from 0% to min (13.04%, 17.65%), or 0% -13%.

To further assess the overall comparability between the readings of C and M delimited by FDA's requirement, a success is defined if a D value falls within 0%-13%, or a failure if D is greater than 13%. The overall comparability can then be defined by PD, the proportion of success.

In the statistical analyses, the continuous data and the binary data were summarized by the mean or the proportion, respectively, and their 95% confidence interval (CI). Although we are mainly interested in the outcome comparison among the finger pressures, we also performed the analysis in the old fashion which ignores the pressure factor as conducted in the past studies. To account for the clustering effect of multiple reading within a subject, the Mixed-effect Gamma regression was performed. The test of the 100% comparability was performed through the null hypothesis of binomial proportion of 1. The bar charts were used to depict the influence of the factors which might have the impact on D, viz., the percentage uncertainty of K, because the factors of concern in this study are the finger pressures and the finger recovery status.

4. Results and discussion

4.1 Spectrum extraction and analysis

The spectrum of one subject under different contact pressures was shown below. Y axis of the spectrum is the absorption of infrared light and the X axis represents the wavenumber, which equals to the reciprocal of the wavelength. After the spectral test, the

blood glucose level of such subject was measured by glucometer. The peak around 1080 cm-1 was selected to be analyzed because it is the unique absorption peak of glucose which is contributed by the vibration of the ether bond (Kino S., 2016).

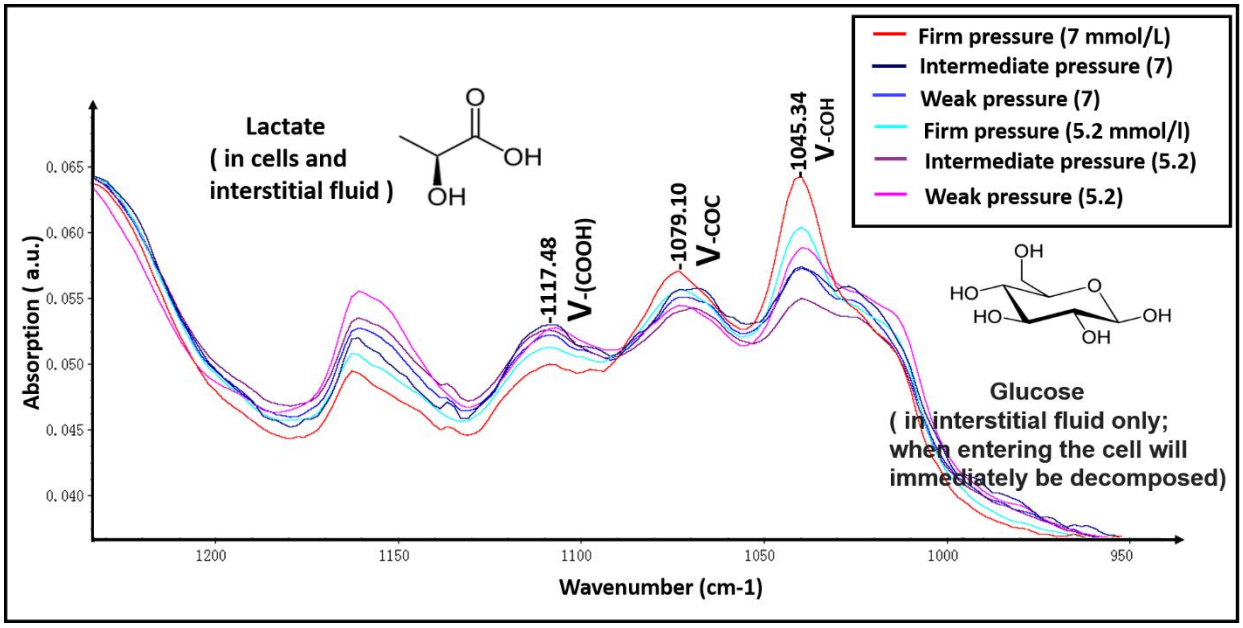

Figure 12 The spectrum of one subject under different pressures

According to the literature review (Kino S., 2016; Eikje, N. S., 2007; Jerônimo, D. P., 2012; Kasahara, R., 2018), some methods were used to extract the absolute peak area such as Gaussian distribution or directly picking the peak height as the absorption value. However, these methods are not appropriate in our case since unlike the quantum cascade lasers (QCL), the baseline of the normal spectrometer is not always reliable. When electrical power supplies to the filament of halogen lamp in the spectrometer, most of it is converted to thermal energy. Such energy is then absorbed by molecules and intensified

the molecular vibrational level. The photon was therefore generated when the molecules changed back to their original vibrational level and thus emitted infrared light. However, the thermal energy is influenced by the resistance of filament, which is affected by temperature. With the work time increased, the temperature of filament increased accordingly, changed the resistance and influenced the input of thermal energy, thus fluctuated the output of infrared light, which makes the baseline settled as the X axis is not reliable at all.

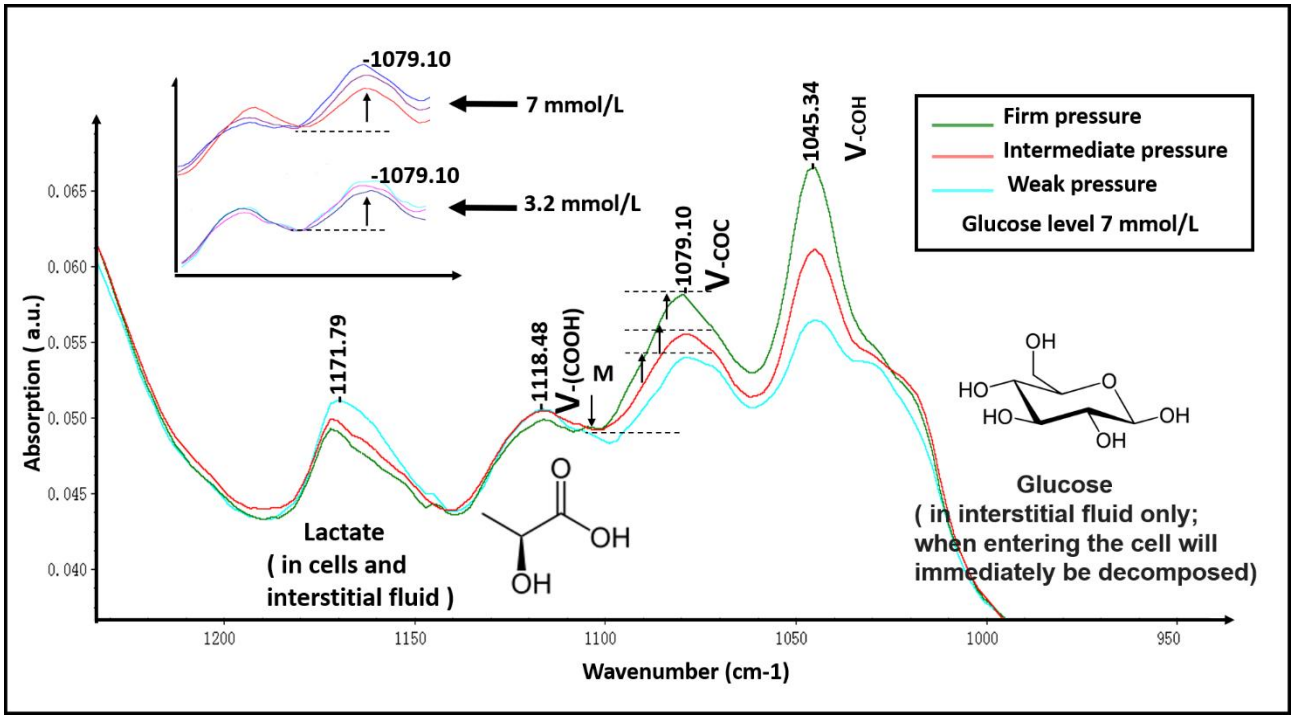

Figure 13 Processed spectrum of one subject under different pressures

Hence, other methods were employed, which settled new reference point or reference line then calculated the relative absorption peak area or height. One common method is selecting the two near troughs of the target peak as the reference and integrated the area in between. Nevertheless, in our spectrum, it can be seen that the position of the right trough near our target peak 1080 cm-1, was changed under various contact pressures. The change of this trough is caused by the 1045 cm-1 peak difference which is considered to be the vibration of carbon oxygen bond of glucose and other components and is influenced by various pressures. Thus, the trough around 1045 cm-1 is not reliable to be a decent reference point. Compared with the 1045 cm-1 trough, the left trough around 1100 cm-1 is stabilised even when the pressure was varied. It is because the peak at 1118 cm-1 was considered to be the vibration of carbonyl bond of lactate (Hackett J., 2016). As shown in the figure, glucose has both cyclic form (α-glucose and β-glucose) and linear form (γ-glucose). However, due to the unstable of the linear γ-glucose, blood glucose molecules barely existed in such form. More than 99.99% glucose molecules existed as the α-glucose and β-glucose (Park, S., 2006; Wang, G., 2013). Thus, the absorption peak at around 1118 cm-1 is barely influenced by the glucose concertation since nearly none of them contained the carbonyl bond. Besides, the concentration level of lactate in human body remains stable if people do not engage in fierce physical activities. It is therefore the trough around 1100 cm-1 could be the only choice as the reference point in our case. The different value between the peak height of 1080 cm-1 and the left trough at 1100 cm-1 was calculated to be the relative absorption of glucose. Finally, the relationship between

the absorption and glucose concentration could be established and further analysis of the uncertainty of K could be calculated accordingly.

It can seen that after adjusting of the original spectrum, the relationship between the contact pressure and the BG level reveals more clear. As shown in Figure 13, with the increase of the contact pressure, the relative peak height of 1080 cm-1 increases accordingly. And also, under the same pressure, the low BG level always gave a smaller relative peak height value compared with the high BG level case.

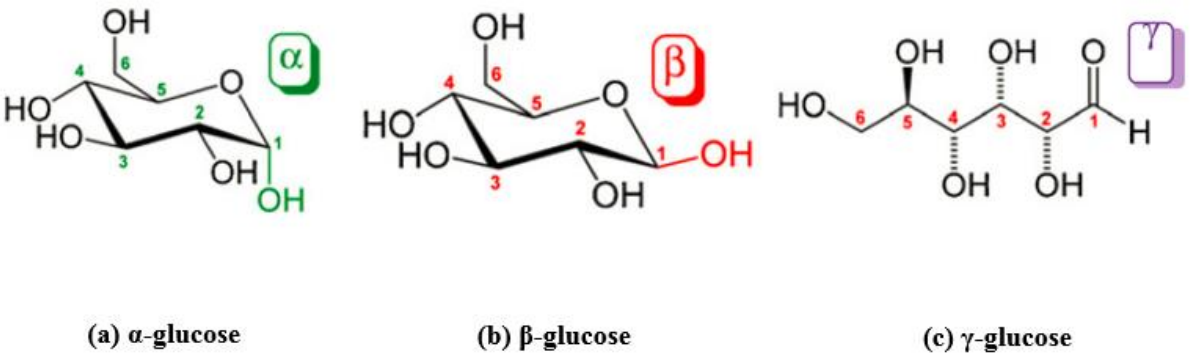

Figure 14 the structure of glucose anomers (Park S, 2006)

Generally, the basic characteristics of a biosensor or a sensing system include sensitivity, selectivity, stability, limit of detection and response time. Sensitivity is the ability of a certain method or a biosensor to distinguish between two very close concentrations and it could be defined by the slope of the detection curve, which means the value of k in our case. And it is shown that with the growth of the contact pressure, the absorbance of glucose increases, which means the higher contact pressure gives better

sensitivity. Selectivity is the ability of a biosensor or a sensing system to measure a concentration of one particular substance in presence of other components. In our case, due to the unique absorption of ether bond for glucose only at peak 1080 cm-1, the selectivity of our sensing method is satisfied. The stability of our method is satisfied since it's based on the ATR spectral measurement which has no decomposition problems compared with the chemically synthesized biosensors. The limit of detection (LOD) could be defined as the lowest quantity or concentration of a certain component or substance that can be detected reliably with a given measuring method. In our case, the LOD is not clear right now because the lowest blood glucose concentration of our employed subjects is 3.2 mmol/L. However, it could still be calculated by the relationship of the signal and noise. Because the limitation of normal human's blood glucose level, subjects with hypoglycemia will be considered for our further research. The response time of our case equals to the scanning time of the spectrum, which is about only 12 seconds. It can be easily seen from the figure 15 that the absorption of glucose grows when the contact pressure changed from weak to firm, which represents the sensitivity of our method improved with the increase of the contact pressure.

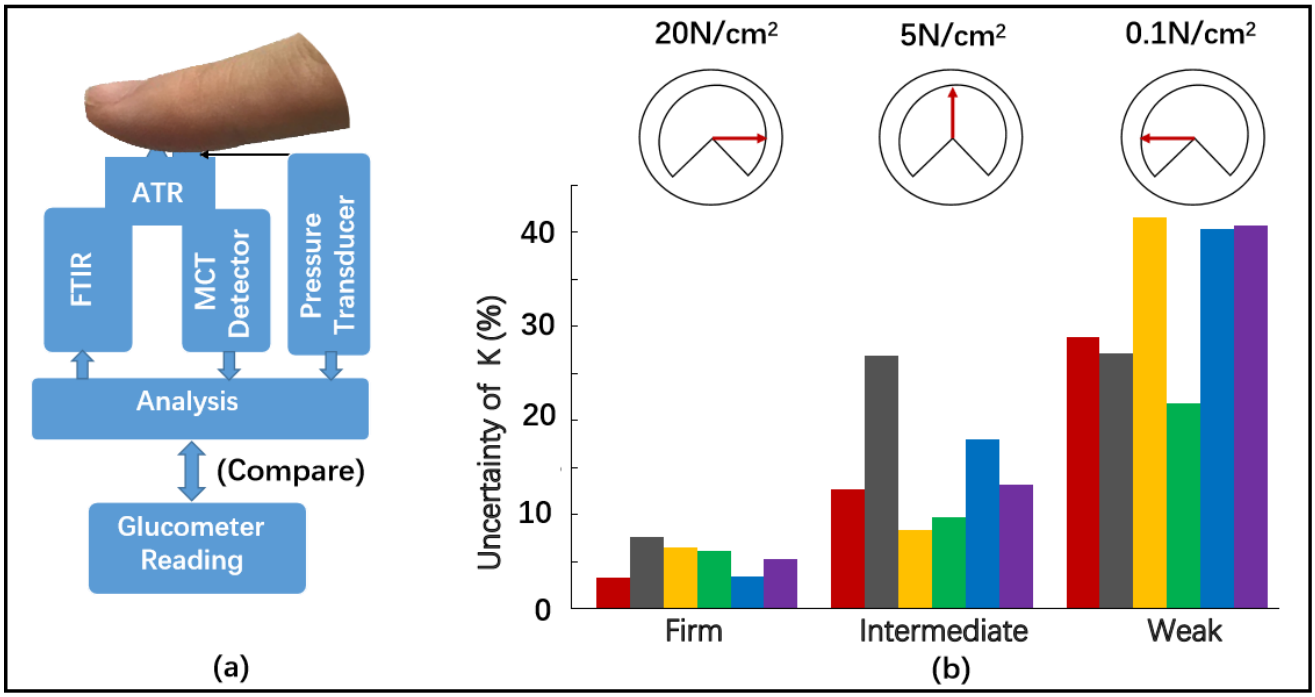

Figure 15 (a) schematic illustration of the experimental procedure; (b) sketch of the percentage uncertainty of K under variable pressure

With the addition of the pressure transducer, the glucose level in the human interstitial fluid was probed by Mid-IR in a usual manner, through the measurement of peak height (M), which was then compared with the "true" glucose concentration (C), determined by an invasive glucose meter. The resulting association coefficient (K=M/C) was then analyzed to obtain the accuracy of the Mid-IR technique while incorporating the factor of contact pressure at different levels. A brief overview for a number of participants with varying finger contact pressure, is shown in Figure 15, where the mean percentage uncertainty of K drops below 8% consistently across the subjects at a firm contact pressure of about 20 N/cm2, whereas it becomes several times larger at

intermediate and weak contact pressures. Correspondingly, the Mid-IR accuracy fluctuates at 58-81% for the lower pressures but increases to 92%-97% for the firm pressure measurement, surpassing for the first time the long-setting target of FDA.

4.2 Statistical analysis

When all the observations were collapsed into firm, intermediate and weak pressure groups regardless of subjects, the mean percentage uncertainty of K in the firm pressure group was substantially lower, at 5.05% (95%CI: 3.57%, 6.47%), than the intermediate pressure group and the weak pressure group of 14.59% (95%CI: 9.96%, 19.23%) and 33.95% (95%CI: 23.02%, 44.89%), respectively. The Mixed-effect Gamma regression adjusting the subject's clustering factor confirmed the finding with the unadjusted results as above (Table 1). Conceivably, the accuracy of the Mid-IR technique incorporating a firm finger pressure is well beyond the FDA standard.

Furthermore, we achieved 100% of the time on the comparability between the readings of C and M in firm pressure group as per FDA's standard; whereas 40% (95%CI:18.53%, 61.47%) and 20% (95%CI:2.47%, 37.53%) for intermediate and the weak pressure group, respectively (Table 2). As a result, the distribution of the K uncertainty has to be simulated by the Gamma model since the distribution peaks near the origin, rather than in the middle, and continuously dropping to the right. Moreover, Gamma distribution is relatively assumption-light means of modeling non-negative data,

we therefore used the Mixed-effect Gamma regression adjusting the subject's clustering factor for the adjusted analysis.

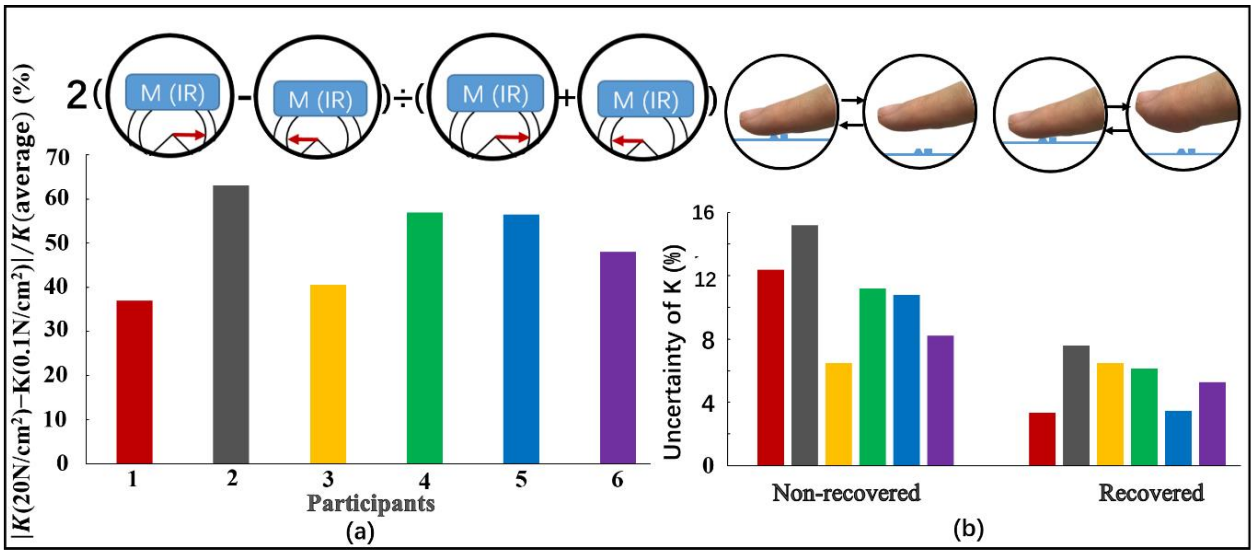

Figure 16 (a) K variation by pressure change; (b) uncertainty of K (non-recovered vs recovered)

Table 1 Percentage uncertainty of K

Pressure level	Unadjusted estimate (95%CI)	Adjusted estimate* (95%CI)
Firm (n=15)	5.05% (3.57%, 6.47%)	5.02% (3.58%, 7.03%)
Intermediate (n=20)	14.59% (9.96%, 19.23%)	14.53% (10.86%, 19.45%)
Weak(n=20)	33.95% (23.02%, 44.89%)	33.94% (25.35%, 45.43%)
Aggregated (n=55)	19.02% (13.81%, 24.24%)	19.02% (13.38%, 27.04%)

*by Mixed–effect Gamma regression analysis

Table 2 Overall comparability

Pressure level	P_D (95%CI)	p-value (H_0: p=1) *
Firm (n=15)	100% (100%, 100%)	0.99
Intermediate (n=20)	40% (18.53%, 61.47%)	< 0.0001
Weak (n=20)	20% (2.47%, 37.53%)	< 0.0001
Aggregated (n=55)	49% (38.55%, 62.30%)	< 0.0001

*test null proportion of 1, i.e., 100% meet FDA's requirement.

The pressure dependence of K uncertainty can be further elucidated by Fig. 16 (a), where the ratios of |K(20N/cm2)-K(0.1N/cm2)| over K(average) have been plotted for 6 participants together with their blood sugar variations. Even without PLSR data analysis, it is already clear that, K not only changes tremendously by pressure variation, but also differs from person to person. On average, K values increase up to 60% when the pressure drops from 20 to 0.1 N/cm2, not only confirming that a higher pressure is always favourable for a larger Mid-IR reading M, but also revealing that the amount of favour

brought in is also dependent upon each individual. Obviously, all this implies the missing pressure indicator has been the very reason why the accuracy has been staggering below 75-80% to this day.

It is therefore necessary to incorporate the pressure indicator in the measurement and the data analysis, as well as to distinguish the K analysis of each individual. Compared with the previous attempts, one finds that, the usual Mid-IR measurements not only disregarded pressure sensing, thus leading to the mixed-up of possible firm, intermediate and weak pressure results, but also ignored the dependence of K upon each individual, resulting in the blending data from different people, which jeopardizes further the accuracy of the whole technique, in spite of the tedious PLSR process added on top. Our study confirms the low accuracy in the mean percentage uncertainty of K of 19.02% (95%CI: 13.81%, 24.24%) if we blended data together, ignoring the finger pressure factor (Table 1). In terms of the comparability between the readings of C and M, the result in the blended group was 49% (95%CI: 38.55%, 62.30%), which was less than half the chance of success (Table 2). In the meantime, although the K accuracy increases with the pressure, it is also found that, when the contact pressure reaches a certain level, the improvement in accuracy will become less evident, or, the percentage uncertainty of K becomes insensitive to the pressure change by then.

Another interesting observation related to all this has been the finger recovery. It was found that after each firm contact pressure Mid-IR measurement, the finger needs to be “recovered” from the pressuring state, before taking the second acquisition, or the result would be jeopardized to some extent. Fig. 16 (b) demonstrated the uncertainties of

K with and without recovery across the subjects differ significantly, revealing that such uncertainty will be increased dramatically if not recovered. Collapsed with the "non-recovered" data in the firm pressure group, the mean percentage uncertainty of K (D) increased to 8.94% (95%CI: 5.16%, 12.69%) and the overall comparability decreased to 75% (95%CI: 56%, 94%).

As this is the first study investigating the finger pressure effect on the Mid-IR measures, we don't have the previous data for the sample size estimation prior to the experiment. As an initial attempt, we employed 6 subjects. Nevertheless, given the highly significant effect of the estimate, as well as the very narrow 95% confidence interval, we realize the results are conclusive for the firm finger pressure group. And there is no need to carry out the retrospective power analyses, as it is not recommended in the practice.

4.3 Bland-Altman analysis

To illustrate the accuracy under various pressures, the Bland-Altman analysis is employed, as shown in Fig. 17. It is clear that, with rising pressure, the range of 95% confidence interval is getting narrower, from [5.3, -5.9] under weak pressure, to [2.1, -2.2] under intermediate pressure, and finally to [0.73, -0.77] under firm pressure. Moreover, the mean of the difference between predicted values and reference values decreases at the same time, from -0.3 to -0.1 and finally to -0.02. Both illustrate that the accuracy increases dramatically when the pressure grows.

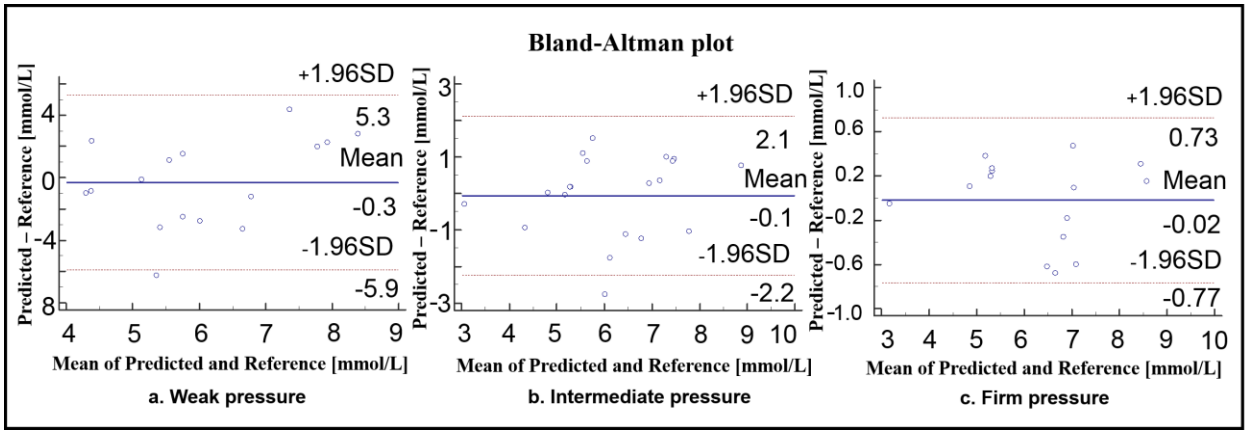

Figure 17 Bland-Altman analysis

4.4 Clarke error grid analysis

Besides, the Clarke error grid analysis is shown in Fig. 18. The Clarke Error Grid Analysis was established in 1987 to quantify the clinical accuracy of diabetic patient estimates or prediction value of their current blood glucose level by a new method as compared to the blood glucose level measured by their glucometers (Clarke W. L., 1987). Eventually, it is considered as one of the "gold standards" for illustrating the accuracy of the new method for monitoring blood glucose level. Values within Region A means the inaccuracy is within 20%, Region B represents the inaccuracy of the new method is outside of 20% but will not lead to unnecessary treatment. Region C, D, E are medically unacceptable. Region C leads to inappropriate treatment, Region D indicates a potential

failure to detect hypoglycemia or hyperglycemia for patients, and Region E provides the ambiguous data for the treatment of hypoglycemia for hyperglycemia.

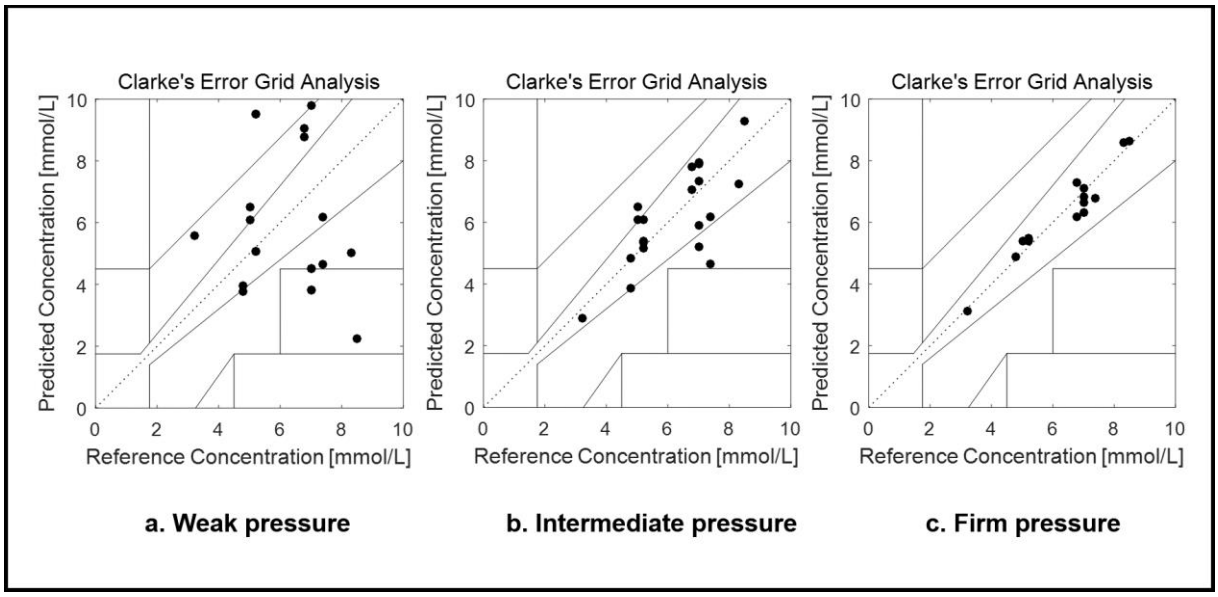

Figure 18 Clarke error grid analysis

With the increase of pressure, points become more concentrated and all of them locate in the central area under the firm pressure, which demonstrates that, predicted values become more precise and eventually achieve the extraordinary accuracy under the firm pressure.

4.5 Rationale

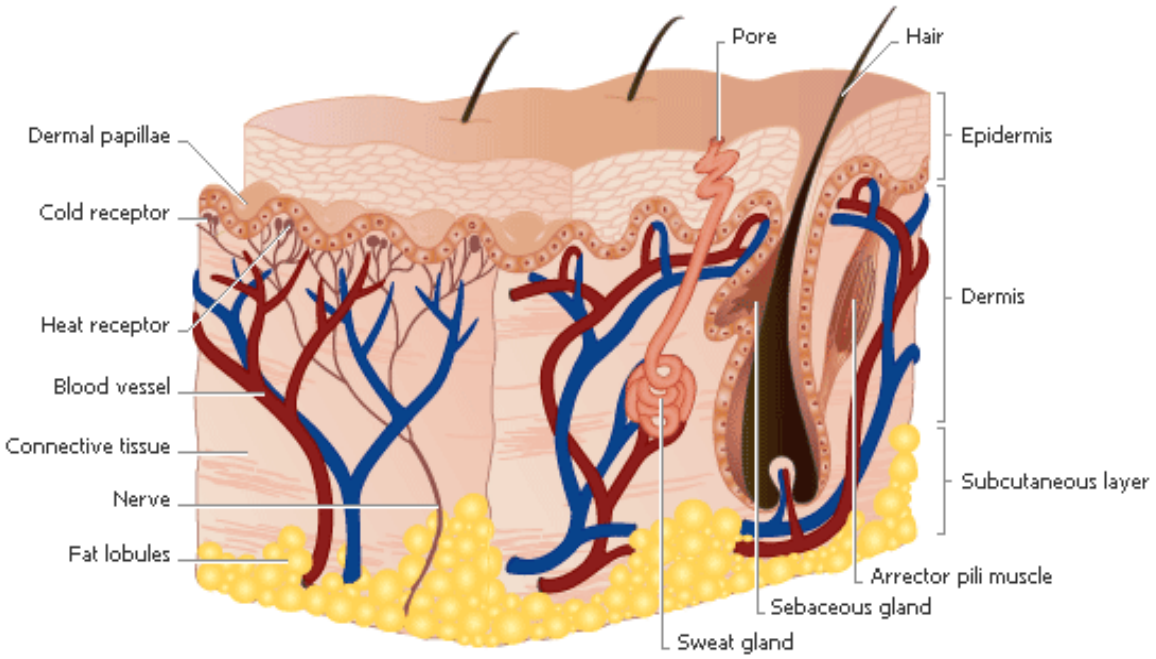

Figure 19 Structure of human skin (Martin N.,2016)

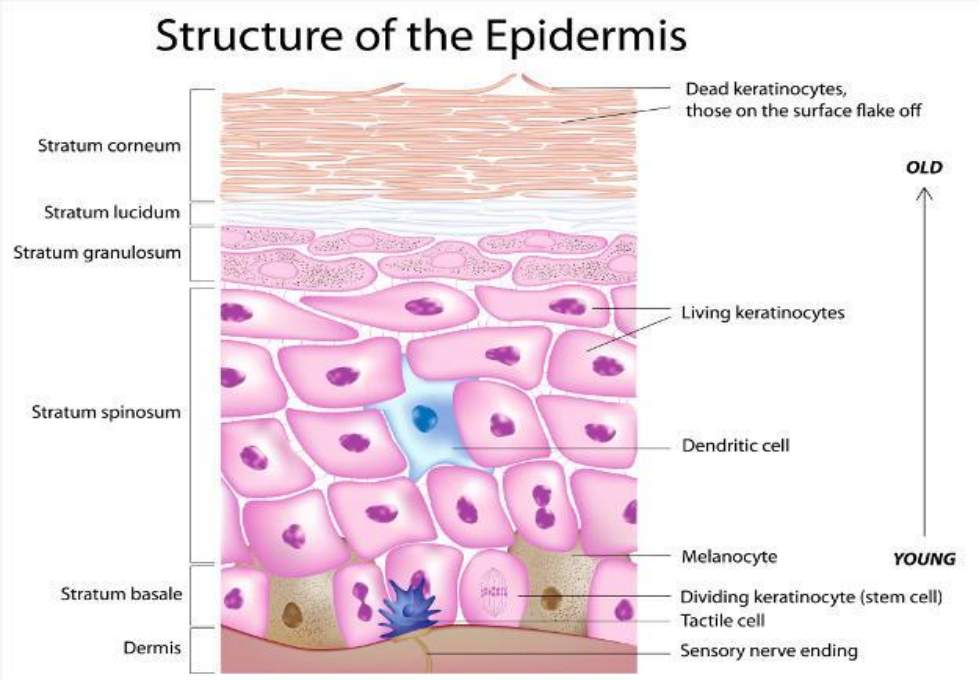

Figure 20 Structure of the epidermis (Martin N.,2016)

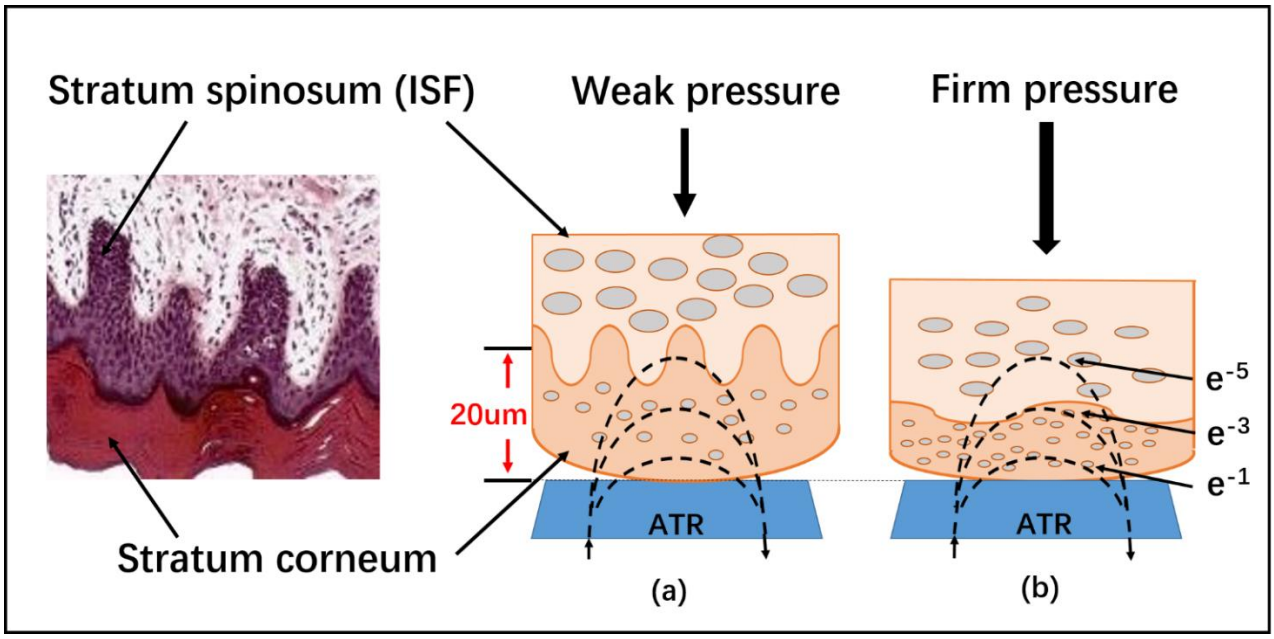

Figure 21 (a) human epidermis under weak pressure (Martin N.,2016); (b) human epidermis under firm pressure

The above observation in fact helps to explain why the contact pressure is a critical variable in the entire scheme here. Following the anatomy of a fingertip, the tissue might undergo some morphological change under pressure. As shown in Fig. 21 (a), when a finger is under weak contact pressure, the interface between the dead cells of stratum corneum and stratum spinosum is not planar but intertwined. It is well known that ISF can only be found beneath the stratum spinosum, thus hard to be reached by the Mid-IR beam in this scenario, as the penetration length of ATR is about 5 micrometers, only ¼ of the stratum corneum thickness (Fig.21a). When a firm contact pressure is applied, however, it will flatten the intertwined interface and homogenize the ISF distribution, which means more ISF can be sensed at the same penetration depth (Fig. 21b). This will

obviously reduce the error of K and hence improve the accuracy. This is not equivalent to, or achievable by the enhancement of the IR power input, which would otherwise be harmful to the living cells.

To a certain extent, the K accuracy enhancement with an increasing pressure could also be related to the effect of ion channels on the surface of cell membrane. Such channels are pressure sensitive, especially for the Na+ and K+ channels. This means when a firm pressure is applied on the finger, the Na+ ion channel of the cell membrane will be closing off, and therefore the Na+ concentration in ISF drops rapidly over time, which alters the Mid-IR absorption. However, the major part of K accuracy enhancement is still believed to be caused by the finger tissue morphological change, as described in Fig. 21, due to the low percentage of sodium contribution.

5. Conclusion

In summary, we have successfully resolved the long-standing problem, to raise the accuracy above the FDA threshold, for the non-invasive blood glucose monitoring by Mid-IR spectroscopy. Our experiments demonstrated the influence of finger contact pressure on the resulting data, which explains why a satisfactory accuracy could not be attained before. Pressure sensing or control, which was neglected but easily achieved, was found to be the key to the enhancement of the accuracy, which can now be raised above

95%. The previous works resulted in only about 70% accuracy on average, barely hitting 80+%, whereas ours reaches 95%, finally exceeding the requirement of FDA. Based on the simple picture of anatomy, we are also able to provide a brief explanation of the skin-deep phenomenon.

Further development on the fitting pressure sensors, adapting ring-shaped rather than a disc for example, or automating pressure application, will certainly allow for the commercialization of the practical non-invasive glucose meters employing portable Mid-IR spectroscopy, alleviating 400+ million diabetes mellitus patients from painful and invasive blood glucose test. Moreover, similar ideas may be extended to the non-invasive examination of other human substance, such as, blood lipids, or even various proteins, which will benefit the research as well as the possible early diagnosis in many areas.

6. Future work

As mentioned before, our experiments demonstrated the influence of finger contact pressure on the resulting data, which explains why a satisfactory accuracy could not be attained before. Pressure sensing or control, which was neglected but easily achieved, was found to be the key to the enhancement of the accuracy. The further development we would like to do is to find out the optimum pressure for higher accuracy, and others will lead to a decrease in accuracy. Moreover, based on the simple picture of anatomy, we are able to provide a brief explanation of the skin-deep phenomenon, which

we will also focus on in the next step, trying to give a more detailed explanation and experimental proof for our theory.

Fig. 18. A Human skin sample from Genoskin (Genoskin, 2019)

In order to verify our two hypotheses as mentioned before, experiments have been designed. Human skin samples could be purchased from Genoskin Company. The samples have complete structures which contain all layers of normal human skins. And all these samples keep alive in Genoskin's patented matrix, which means they could offer real response of live human skins.

The samples will be separated into two groups. Group 1 is the original samples, group 2 is the samples added sodium channel inhibitors into the matrix, which could close

off the sodium ion channels and has the equal effect to the influence of pressure. Both groups' samples remain the same glucose level in the original matrix. In addition, ATR mid-infrared probe could be put on one of each group's samples and spectrums could be obtained. Then, the same pressure regulated by pressure sensor could be applied on samples of each group and the spectrums of these pressured samples could be obtained. After the spectral measurement of each group' s samples, 95% alcohol solution would be added into the matrix, which would kill cells immediately and fix the skin structure in all scenarios. After that, methacrylate would be added for infiltrating and supporting samples, avoiding the mechanical influence of skin structure when cutting into cross-section specimens by rotary microtome. After dyeing and cutting procedure, we could compare the structure of skins with or without pressure.

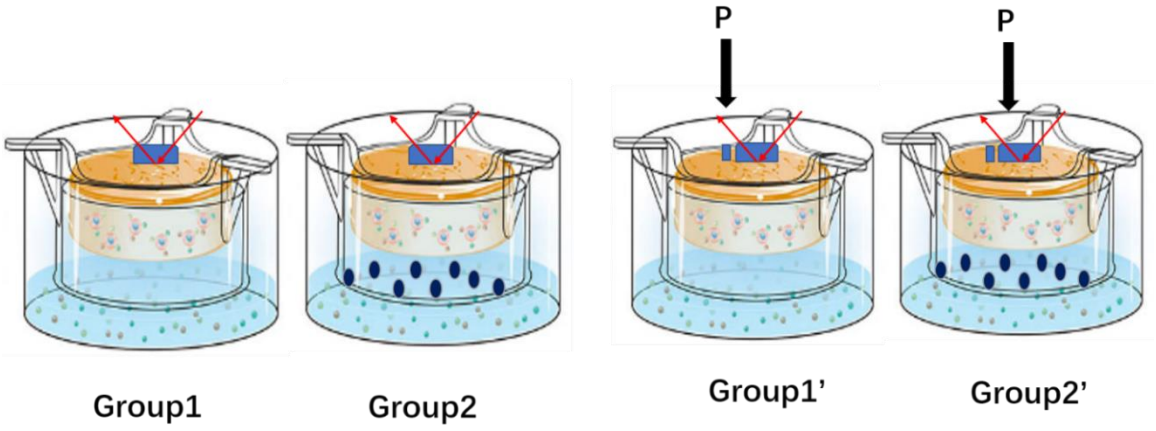

Fig. 19. Spectral measurements of different scenarios

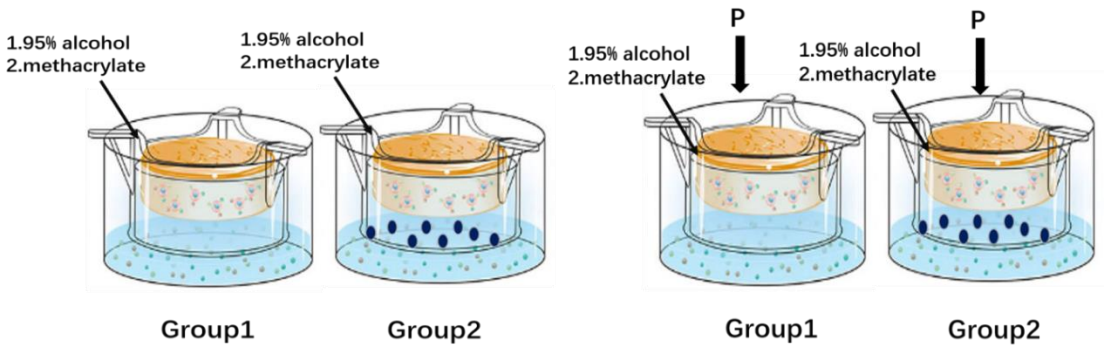

Fig. 20. Preparation before cutting

If the absorption of glucose is different between group 1 and 2, it indicates the changes of ion channels have influence of the spectrum of glucose absorption. If the absorption of glucose on spectrum is the same in both groups, then the hypothesis about ion channels is not correct. After discussing the influence of ion channels, we could discuss the influence of pressure on human skin's structure. If the absorption of glucose on spectrum is different with or without pressure in group 2, our hypothesis that the skin structure has been changed by pressure could be discussed further. If we could observe the structure of skin samples changing from zigzag to be smoother under pressure, then the structural change could be the reason for different absorption of glucose under various pressures. However, if the absorption is different between group 1 and 2, also varied with or without pressure, then it indicates both the skin structure change and ion channels have influence on the absorption of glucose.

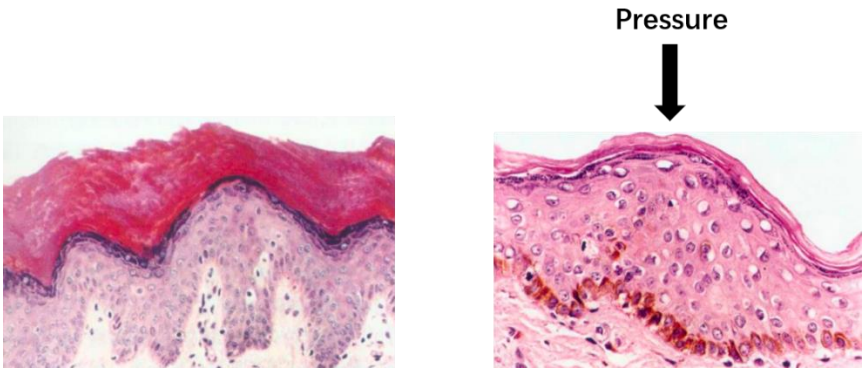

Fig. 21. Expected change of skin structure (Martin N.,2016)

Another interesting phenomenon we found is that when the glucose concentration increases, the 1080 cm-1 peak became higher but thinner. However, in the aqueous glucose solution, we didn't observe such a phenomenon happened, which indicates that the intermolecular bond of glucose itself is not the reason for this phenomenon. Thus, the dipole-dipole interaction or intermolecular bond between glucose and other ISF components could be considered and analyzed separately. After finding out the reason we would try to build a correlation between the components concertation and quantize the influence of such interaction phenomenon on the absorption peak. Then, the traditionally existing area extraction method based on Gaussian-distribution could be modified by adding the changes of such phenomenon, which makes it more accurate and could be also considered for other spectral analysis of mixed solutions.

What's more, we found that some other parts of the human body could be a better experimental position since it may not have the stratum corneum layer. The stratum

corneum layer only contains dead cells. It is a hindrance to detect glucose since it has no interstitial fluid which can directly reflect the glucose level in the human body.

Besides, to overcome the limitation of the near infrared method, whose absorption peak is seriously influenced by water and other components, some new strategies could be studied the next. It is known that the pulse oximeter has been used as practical products for many years, which is precisely accurate. Its principle is similar to the blood glucose measurement by infrared, which analyzes the absorption of two types of hemoglobin (loaded or unloaded oxygen) to calculate oxygen content. Glucose has an absorption peak at around 950 nm and is considered to be the least affected by other substances. However, the problem is that the intensity of such peak is very weak and sometimes difficult to be shown on the spectrum when doing an in-vivo test. The error will increase accordingly if the peak becomes more clear when some spectral processing methods are employed, such as the second derivative method. Hence, peaks of hemoglobin could be used for calibration, since the measurement accuracy of such substance has been proved to be excellent. Thus, a calibrated model could be built based on the absorption at 950 nm.

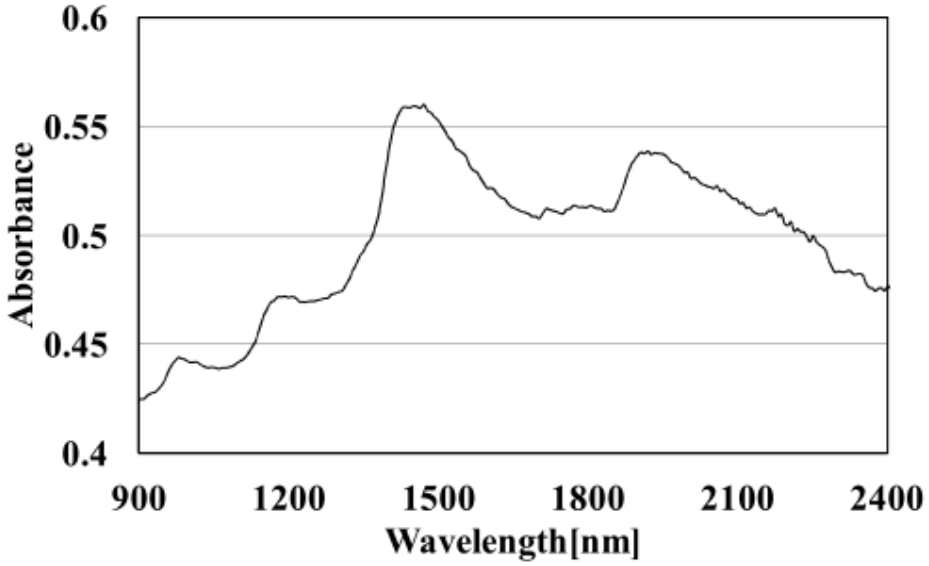

Fig. 22. NIR spectrum of glucose aqueous solution (Yoshinari H., 2012)

Moreover, genetic algorithms could be applied for selecting the optimum wavelengths area. It could be started from the specific spectral region barely influenced by water. Each wavelength can be established as an absorption model separately by configuring different aqueous solutions. Wavelengths with less accuracy will be eliminated. Then hemoglobin, albumin, serum, etc. could be gradually added to the aqueous to simulate the in-vivo environment. Finally, the optimum wavelengths could be screened out and applied in practice.

References

Renard, E., 2005. Monitoring glycemic control: the importance of self-monitoring of blood glucose. *The American journal of medicine*, *118*(9), pp.12-19.

Diabetes Control and Complications Trial Research Group. (1993). The effect of intensive treatment of diabetes on the development and progression of long-term complications in insulin-dependent diabetes mellitus. *N Engl j Med*, *1993*(329), 977-986.

O Connell, P.J., Hawthorne, W.J., Holmes-Walker, D.J., Nankivell, B.J., Gunton, J.E., Patel, A.T., Walters, S.N., Pleass, H.C., Allen, R.D. and Chapman, J.R., 2006. Clinical islet transplantation in type 1 diabetes mellitus: results of Australia's first trial. *Medical journal of Australia*, *184*(5), p.221.

Tao, Z., Shi, A. and Zhao, J., 2015. Epidemiological perspectives of diabetes. *Cell biochemistry and biophysics*, *73*(1), pp.181-185.

Saptari, V. A. (2004). *A spectroscopic system for near infrared glucose measurement* (Doctoral dissertation, Massachusetts Institute of Technology).

World Health Organization, 2016. *Evaluation of Certain Food Additives and Contaminants: Eightieth Report of the Joint FAO/WHO Expert Committee on Food Additives* (Vol. 80). World Health Organization.

Aguiree, F., Brown, A., Cho, N.H., Dahlquist, G., Dodd, S., Dunning, T., Hirst, M., Hwang, C., Magliano, D., Patterson, C. and Scott, C., 2013. IDF diabetes atlas.

Risérus, U., Willett, W.C. and Hu, F.B., 2009. Dietary fats and prevention of type 2 diabetes. *Progress in lipid research*, *48*(1), pp.44-51.

Yadav, J., Rani, A., Singh, V. and Murari, B.M., 2015. Prospects and limitations of non-invasive blood glucose monitoring using near-infrared spectroscopy. *Biomedical signal processing and control*, *18*, pp.214-227.

Baehr, P.H. and McDonald, G.B., 1994. Esophageal infections: risk factors, presentation, diagnosis, and treatment. *Gastroenterology*, *106*(2), pp.509-532.

DCCT Research Group, 1993. Diabetes Control and Complications Trial (DCCT): the effect of intensive treatment of diabetes on the development and progression of long-term complications in insulin-dependent diabetes mellitus. *N Engl J Med*, *329*(14), pp.977-86.

International Association of Diabetes and Pregnancy Study Groups Consensus Panel, 2010. International association of diabetes and pregnancy study groups recommendations on the diagnosis and classification of hyperglycemia in pregnancy. *Diabetes care*, *33*(3), pp.676-682.

Centers for Disease Control and Prevention, 2011. National diabetes fact sheet: national estimates and general information on diabetes and prediabetes in the United States, 2011. *Atlanta, GA: US Department of Health and Human Services, Centers for Disease Control and Prevention*, *201*(1).

Rathmann, W. and Giani, G., 2004. Global prevalence of diabetes: estimates for the year 2000 and projections for 2030. *Diabetes care*, *27*(10), pp.2568-2569.

Chase, H.P., Beck, R.W., Xing, D., Tamborlane, W.V., Coffey, J., Fox, L.A., Ives, B., Keady, J., Kollman, C., Laffel, L. and Ruedy, K.J., 2010. Continuous glucose monitoring in youth with type 1 diabetes: 12-month follow-up of the Juvenile Diabetes Research

Foundation continuous glucose monitoring randomized trial. *Diabetes technology & therapeutics*, *12*(7), pp.507-515.

Yadav, J., Rani, A., Singh, V. and Murari, B.M., 2015. Prospects and limitations of non-invasive blood glucose monitoring using near-infrared spectroscopy. *Biomedical signal processing and control*, *18*, pp.214-227.

Buckingham, B., Block, J. and Wilson, D.M., 2005. Continuous glucose monitoring. *Current Opinion in Endocrinology, Diabetes and Obesity*, *12*(4), pp.273-279.

Rhee, S.Y., Chon, S., Koh, G., Paeng, J.R., Oh, S., Woo, J.T., Kim, S.W., Kim, J.W. and Kim, Y.S., 2007. Clinical experience of an iontophoresis based glucose measuring system. *Journal of Korean medical science*, *22*(1), pp.70-73.

Heinemann, L., 2003. Continuous glucose monitoring by means of the microdialysis technique: underlying fundamental aspects. *Diabetes technology & therapeutics*, *5*(4), pp.545-561.

Bolincier, J., Ungerstedt, U. and Arner, P., 1992. Microdialysis measurement of the absolute glucose concentration in subcutaneous adipose tissue allowing glucose monitoring in diabetic patients. *Diabetologia*, *35*(12), pp.1177-1180.

Renard, E., 2008. Implantable continuous glucose sensors. *Current diabetes reviews*, *4*(3), pp.169-174.

Vaddiraju, S., Tomazos, I., Burgess, D.J., Jain, F.C. and Papadimitrakopoulos, F., 2010. Emerging synergy between nanotechnology and implantable biosensors: a review. *Biosensors and Bioelectronics*, *25*(7), pp.1553-1565.

Wentholt, I.M., Vollebregt, M.A., Hart, A.A., Hoekstra, J.B. and DeVries, J.H., 2005. Comparison of a needle-type and a microdialysis continuous glucose monitor in type 1 diabetic patients. *Diabetes Care*, *28*(12), pp.2871-2876.

Tura, A., Maran, A. and Pacini, G., 2007. Non-invasive glucose monitoring: assessment of technologies and devices according to quantitative criteria. *Diabetes research and clinical practice*, *77*(1), pp.16-40.

Chuang, H., Taylor, E. and Davison, T.W., 2004. Clinical evaluation of a continuous minimally invasive glucose flux sensor placed over ultrasonically permeated skin. *Diabetes technology & therapeutics*, *6*(1), pp.21-30.

Vashist, S.K., 2013. Continuous glucose monitoring systems: a review. *Diagnostics*, *3*(4), pp.385-412.

Christiansen, M., Bailey, T., Watkins, E., Liljenquist, D., Price, D., Nakamura, K., Boock, R. and Peyser, T., 2013. A new-generation continuous glucose monitoring system: improved accuracy and reliability compared with a previous-generation system. *Diabetes technology & therapeutics*, *15*(10), pp.881-888.

Garg, S.K., Smith, J., Beatson, C., Lopez-Baca, B., Voelmle, M. and Gottlieb, P.A., 2009. Comparison of accuracy and safety of the SEVEN and the Navigator continuous glucose monitoring systems. *Diabetes technology & therapeutics*, *11*(2), pp.65-72.

Weinstein, R.L., Schwartz, S.L., Brazg, R.L., Bugler, J.R., Peyser, T.A. and McGarraugh, G.V., 2007. Accuracy of the 5-day FreeStyle navigator continuous glucose monitoring system. *Diabetes Care*, *30*(5), pp.1125-1130.

Block, C.D., Manuel-y-Keenoy, B. and Van Gaal, L., 2008. A review of current evidence with continuous glucose monitoring in patients with diabetes.

Eikje, N.S., Sota, T. and Aizawa, K., 2007, June. Cutaneous approach towards clinical and pathophysiological aspects of hyperglycemia by ATR FTIR spectroscopy. In *European Conference on Biomedical Optics* (p. 6628_63). Optical Society of America.

Kino, S., Omori, S. and Matsuura, Y., 2016, March. Blood glucose measurement in vivo using hollow-fiber based, mid-infrared ATR probe with multi-reflection prism. In *SPIE BiOS* (pp. 970209-970209). International Society for Optics and Photonics.

Liakat, S., Bors, K.A., Xu, L., Woods, C.M., Doyle, J. and Gmachl, C.F., 2014. Noninvasive in vivo glucose sensing on human subjects using mid-infrared light. *Biomedical optics express*, *5*(7), pp.2397-2404.

Yao, H., et al., 2011. A contact lens with embedded sensor for monitoring tear glucose level. *Biosensors and Bioelectronics*, *26*(7), pp.3290-3296.

Chu, M.X., Miyajima, et al., 2011. Soft contact lens biosensor for in situ monitoring of tear glucose as non-invasive blood sugar assessment. *Talanta*, *83*(3), pp.960-965.

Iguchi, S., Kudo, et al., 2007. A flexible and wearable biosensor for tear glucose measurement. *Biomedical microdevices*, *9*(4), pp.603-609.

Kino S, et al., 2016. Blood glucose measurement in vivo using hollow-fiber based, mid-infrared ATR probe with multi-reflection prism. *InOptical Fibers and Sensors for Medical Diagnostics and Treatment Applications XVI*.

Jerônimo, Diego Pereira, et al. "Detection of creatine in rat muscle by FTIR spectroscopy." *Annals of biomedical engineering,* 40.9 (2012): 2069-2077.

Kasahara, Ryosuke, et al. "Noninvasive glucose monitoring using mid-infrared absorption spectroscopy based on a few wavenumbers." *Biomedical optics express*. 9.1 (2018): 289-302.

Liakat S, et al., 2014. Noninvasive in vivo glucose sensing on human subjects using mid-infrared light. *Biomedical optics express.* 5(7), pp.2397-404.

Sen, D.K. and Sarin, G.S., 1980. Tear glucose levels in normal people and in diabetic patients. *British journal of ophthalmology*, *64*(9), pp.693-695.

Heise, H.M., Bittner, A. and Marbach, R., 1998. Clinical chemistry and near infrared spectroscopy: technology for non-invasive glucose monitoring. *Journal of Near Infrared Spectroscopy*, *6*, pp.349-360.

Vashist, S.K et al., 2011. Technology behind commercial devices for blood glucose monitoring in diabetes management: A review. *Analytica chimica acta*, *703*(2), pp.124-136.

Tura, A., Maran, A. and Pacini, G., 2007. Non-invasive glucose monitoring: assessment of technologies and devices according to quantitative criteria. *Diabetes research and clinical practice*, *77*(1), pp.16-40.

do Amaral, C.E.F. and Wolf, B., 2008. Current development in non-invasive glucose monitoring. *Medical engineering & physics*, *30*(5), pp.541-549.

Ellis, D.I. and Goodacre, R., 2006. Metabolic fingerprinting in disease diagnosis: biomedical applications of infrared and Raman spectroscopy. *Analyst*, *131*(8), pp.875-885.

Vashist, S.K., 2012. Non-invasive glucose monitoring technology in diabetes management: A review. *Analytica chimica acta*, *750*, pp.16-27.

Barman, I., 2011. *Unraveling the puzzles of spectroscopy-based non-invasive blood glucose detection* (Doctoral dissertation, Massachusetts Institute of Technology).

Roychoudhury, P., Harvey, L.M. and McNeil, B., 2006. At-line monitoring of ammonium, glucose, methyl oleate and biomass in a complex antibiotic fermentation process using attenuated total reflectance-mid-infrared (ATR-MIR) spectroscopy. *Analytica Chimica Acta*, *561*(1), pp.218-224.

Shen, Y.C., Davies, A.G., Linfield, E.H., Elsey, T.S., Taday, P.F. and Arnone, D.D., 2003. The use of Fourier-transform infrared spectroscopy for the quantitative determination of glucose concentration in whole blood. *Physics in medicine and biology*, *48*(13), p.2023.

Khalil, O.S., 2004. Noninvasive photonic-crystal material for sensing glucose in tears.

Heise, H.M. and Marbach, R., 1998. Human oral mucosa studies with varying blood glucose concentration by non-invasive ATR-FT-IR-spectroscopy. *Cellular and molecular biology (Noisy-le-Grand, France)*, *44*(6), pp.899-912.

Khalil, S.F., Mohktar, M.S. and Ibrahim, F., 2014. The theory and fundamentals of bioimpedance analysis in clinical status monitoring and diagnosis of diseases. *Sensors*, *14*(6), pp.10895-10928.

Wang, Guangfeng, et al. Non-enzymatic electrochemical sensing of glucose. *Microchimica Acta*. 180.3-4 (2013): 161-186.

Park, S., Boo, H., & Chung, T. D. (2006). Electrochemical non-enzymatic glucose sensors. *Analytica chimica acta*, 556(1), 46-57.

Hackett, Mark J., et al. "Concurrent glycogen and lactate imaging with FTIR spectroscopy to spatially localize metabolic parameters of the glial response following brain ischemia." *Analytical chemistry*. 88.22 (2016): 10949-10956.

Kruse-Jarres JD, Janatsch G, Gless U, Marbach R, Heise HM, 1990. Glucose and other constituents of blood determined by ATR-FTIR-spectroscopy. *Clinical chemistry*. 36(2):401-2.

Yao H, Shum AJ, Cowan M, Lähdesmäki I, Parviz BA, 2007. A contact lens with embedded sensor for monitoring tear glucose level. *Biosensors and Bioelectronics*. 26(7):3290-6.

Chu MX, 2011. Soft contact lens biosensor for in situ monitoring of tear glucose as non-invasive blood sugar assessment. *Talanta*. 83(3):960-5.

Smith A.H., Bates M.N., 1992. Confidence limit analyses should replace power calculations in the interpretation of epidemiologic studies. *Epidemiology,* pp449-452.

Knapp T R., 1996.The overemphasis on power analysis. *Nursing research, 45(6),* pp379-381.

Hoenig J M, Heisey D M., 2001, The abuse of power: the pervasive fallacy of power calculations for data analysis. *The American Statistician, 55(1),* pp 19-24.

Clarke WL, Cox D, Gonder-Frederick LA, Carter W, Pohl SL: Evaluating clinical accuracy of systems for self-monitoring of blood glucose. *Diabetes Care*, 10:622–628,1987.

Yoshinari, Hiroki, et al. "Non-invasive self monitoring of blood glucose system using near-infrared spectroscopy." *Sice Annual Conference (Sice), 2012 Proceedings Of*. IEEE, 2012.

Appendix Source code of Clarke Error Grid Analysis

```
function [total, percentage] = clarke(y,yp)
% CLARKE    Performs Clarke Error Grid Analysis
%
% The Clarke error grid approach is used to assess the clinical
% significance of differences between the glucose measurement technique
% under test and the venous blood glucose reference measurements. The
% method uses a Cartesian diagram, in which the values predicted by the
% technique under test are displayed on the y-axis, whereas the values
% received from the reference method are displayed on the x-axis. The
% diagonal represents the perfect agreement between the two, whereas the
% points below and above the line indicate, respectively, overestimation
% and underestimation of the actual values. Zone A (acceptable)
represents
% the glucose values that deviate from the reference values by ?0% or
are
% in the hypoglycemic range (<70 mg/dl), when the reference is also
within
% the hypoglycemic range. The values within this range are clinically
exact
% and are thus characterized by correct clinical treatment. Zone B
(benign
% errors) is located above and below zone A; this zone represents those
% values that deviate from the reference values, which are incremented
by
% 20%. The values that fall within zones A and B are clinically
acceptable,
% whereas the values included in areas C-E are potentially dangerous,
and
% there is a possibility of making clinically significant mistakes. [1-4]
%
% SYNTAX:
%
% [total, percentage] = clarke(y,yp)
%
% INPUTS:
% y             Reference values (mg/dl)
% yp            Predicted/estimtated values (mg/dl)
%
% OUTPUTS:
% total         Total points per zone:
%               total(1) = zone A,
%               total(2) = zone B, and so on
% percentage    Percentage of data which fell in certain region:
%               percentage(1) = zone A,
%               percentage(2) = zone B, and so on.
%
% EXAMPLE:      load example_data.mat
%               [tot, per] = clarke(y,yp)
%
% References:
```

```
% [1]   A. Maran et al. "Continuous Subcutaneous Glucose Monitoring in
Diabetic
%       Patients" Diabetes Care, Volume 25, Number 2, February 2002
% [2]   B.P. Kovatchev et al. "Evaluating the Accuracy of Continuous
Glucose-
%       Monitoring Sensors" Diabetes Care, Volume 27, Number 8, August
2004
% [3]   E. Guevara and F. J. Gonzalez, "Prediction of Glucose
Concentration by
%       Impedance Phase Measurements,?in MEDICAL PHYSICS: Tenth Mexican
%       Symposium on Medical Physics, Mexico City (Mexico), 2008, vol.
1032, pp.
%       259?61.
% [4]   E. Guevara and F. J. Gonzalez, "Joint optical-electrical
technique for
%       noninvasive glucose monitoring,?REVISTA MEXICANA DE FISICA, vol.
56,
%       no. 5, pp. 430?34, Sep. 2010.
%
% ?Edgar Guevara Codina
% codina@REMOVETHISactus.iico.uaslp.mx
% File Version 1.2
% March 29 2013
%
% Ver. 1.2 Statistics verified, fixed some errors in the display; thanks
to Tim
% Ruchti from Hospira Inc. for the corrections
% Ver. 1.1 corrected upper B-C boundary, lower B-C boundary slope ok;
thanks to
% Steven Keith from BD Technologies for the corrections!
%
% MATLAB ver. 7.10.0.499 (R2010a)
% ------------------------------------------------------------------------
--------

% Error checking
if nargin == 0
 error('clarke:Inputs','There are no inputs.')
end
if length(yp) ~= length(y)
    error('clarke:Inputs','Vectors y and yp must be the same length.')
end
if (max(y) > 400) || (max(yp) > 400) || (min(y) < 0) || (min(yp) < 0)
    error('clarke:Inputs','Vectors y and yp are not in the physiological
range of glucose (<400mg/dl).')
end
% ------------------------- Print figure flag ------------------------
--------
PRINT_FIGURE = true;
% ------------------------- Determine data length ---------------------
--------
n = length(y);
% ------------------------- Plot Clarke's Error Grid ------------------
```

```
--------
h = figure;
plot(y,yp,'ko','MarkerSize',4,'MarkerFaceColor','k','MarkerEdgeColor','k
');
xlabel('Reference Concentration [mmol/L]');
ylabel ('Predicted Concentration [mmol/L]');
title('Clarke''s Error Grid Analysis');
set(gca,'XLim',[0 400/40]);
set(gca,'YLim',[0 400/40]);
axis square
hold on
plot([0 400/40],[0 400/40],'k:')                    % Theoretical
45?regression line
plot([0 175/120],[70/40 70/40],'k-')
% plot([175/120 320/40],[70/40 400/40],'k-')
plot([175/120 10/1.2],[70/40 10],'k-')          % replace 320 with
400/1.2 because 100*(400 - 400/1.2)/(400/1.2) =  20% error
plot([70/40 70/40],[84/40 400/40],'k-')
plot([0 70/40],[180/40 180/40],'k-')
plot([70/40 290/40],[180/40 400/40],'k-')                % Corrected
upper B-C boundary
% plot([70/40 70/40],[0 175/120],'k-')
plot([70/40 70/40],[0 56/40],'k-')                     % replace 175.3
with 56 because 100*abs(56-70)/70) = 20% error
% plot([70/40 10],[175/120 320/40],'k-')
plot([70/40 400/40],[56/40 320/40],'k-')
plot([180/40 180/40],[0 70/40],'k-')
plot([180/40 400/40],[70/40 70/40],'k-')
plot([240/40 240/40],[70/40 180/40],'k-')
plot([240/40 400/40],[180/40 180/40],'k-')
plot([130/40 180/40],[0 70/40],'k-')                   % Lower B-C
boundary slope OK
text(30,20,'A','FontSize',12);
text(30,150,'D','FontSize',12);
text(30,380,'E','FontSize',12);
text(150,380,'C','FontSize',12);
text(160,20,'C','FontSize',12);
text(380,20,'E','FontSize',12);
text(380,120,'D','FontSize',12);
text(380,260,'B','FontSize',12);
text(280,380,'B','FontSize',12);
set(h, 'color', 'white');                    % sets the color to white
% Specify window units
set(h, 'units', 'inches')
% Change figure and paper size (Fixed to 3x3 in)
set(h, 'Position', [0.1 0.1 3 3])
set(h, 'PaperPosition', [0.1 0.1 3 3])
if PRINT_FIGURE
    % Saves plot as a Enhanced MetaFile
    print(h,'-dmeta','Clarke_EGA');
    % Saves plot as PNG at 800 dpi
    print(h, '-dpng', 'Clarke_EGA', '-r800');
end
```

```
total = zeros(5,1);                             % Initializes output
% ------------------------------ Statistics --------------------------
--------
for i=1:n,
    if (yp(i) <= 70 && y(i) <= 70) || (yp(i) <= 1.2*y(i) && yp(i) >=
0.8*y(i))
        total(1) = total(1) + 1;                % Zone A
    else
        if ( (y(i) >= 180) && (yp(i) <= 70) ) || ( (y(i) <= 70) &&
yp(i) >= 180 )
            total(5) = total(5) + 1;            % Zone E
        else
            if ((y(i) >= 70 && y(i) <= 290) && (yp(i) >= y(i) + 110) )
|| ((y(i) >= 130 && y(i) <= 180)&& (yp(i) <= (7/5)*y(i) - 182))
                total(3) = total(3) + 1;        % Zone C
            else
                if ((y(i) >= 240) && ((yp(i) >= 70) && (yp(i) <= 180)))
|| (y(i) <= 175/3 && (yp(i) <= 180) && (yp(i) >= 70)) || ((y(i) >= 175/3
&& y(i) <= 70) && (yp(i) >= (6/5)*y(i)))
                    total(4) = total(4) + 1;% Zone D
                else
                    total(2) = total(2) + 1;% Zone B
                end                             % End of 4th if
            end                                 % End of 3rd if
        end                                     % End of 2nd if
    end                                         % End of 1st if
end                                             % End of for loop
percentage = (total./n)*100;
% ------------------------------------------------------------------------
--------
% EOF
```